CHAPTER 5 PATTERNS OF CORAL BLEACHING RESPONSE IN SUBTROPICAL EASTERN AUSTRALIA: DIFFERENTIAL BLEACHING SUSCEPTIBILITY AND BLEACHING THRESHOLD

5.1 Abstract

Recent severe coral bleaching events that coincided with elevated sweater temperatures have resulted in the global declines in hard coral cover. Current tools for monitoring coral bleaching potential rely on satellite-derived 50-km resolution twice-weekly sea surface temperature (SST) anomalies, which are available through the Reef Check web site. Satellite-derived SSTs were compared with *in situ* data from subtropical reefs in eastern Australian using regression analyses. There was generally low concordance, but finer-scale (4-km) SST was a better predictor of *in situ* temperature throughout the Solitary Islands Marine Park (SIMP), northern New South Wales (NSW) Australia. Between 1990 and 2008, mean yearly seawater temperatures within the SIMP and Lord Howe Island Marine Park (LHIMP) increased by 0.029 and 0.034°C year^{-1}, respectively. Monitoring of seawater temperature and bleaching between 2004 and 2007 in the SIMP and LHIMP showed that a severe bleaching event did not occur during this time; however, low-level bleaching was observed, with significant seasonal and temporal effects. Bleaching susceptibility of dominant coral families including Pocilloporidae, Poritidae, Acroporidae and Dendrophylliidae varied between locations. Bleaching susceptibility was highest in *Porites* spp. at the most offshore island site within the SIMP during summer 2005. Dominant coral species were found to bleach more often at many sites, with clear difference in bleaching susceptibility found between sites, both within and between locations. A review of published estimates of coral bleaching threshold from other locations suggested that the bleaching threshold at 30-31.5°S range between 26.5-26.7°C. This data provides baseline information on bleaching susceptibility in coral families during a period when there were no mass bleaching episodes and can be utilised in the future to compare with coral bleaching responses during periods when seawater temperature exceed bleaching thresholds.

5.2 Introduction

In the previous two chapters the occurrence and virulence of ASWS were shown to be linked to seasonal temperature pattern, with a strong correlation to higher seawater temperatures. Recent literature suggests that abiotic diseases such as mass coral bleaching events may trigger biological diseases such as ASWS, which may be due to: i) a reduction of photosynthates from the coral symbionts; ii) a reduced capacity of the coral host to resist infection from a pathogenic organism; and/or iii) opportunistic microbes may become pathogenic at higher temperatures (Harvell *et al.* 2001; Mydlarz *et al.* 2006; Croquer and Weil 2009; Mydlarz *et al.* 2009). Studies conducted following the 2005 Caribbean bleaching event showed a clear correlation between bleaching extent and disease incidence (Muller *et al.* 2008). Additionally, Croquer and Weil (2009) found that the intensity of bleaching was correlated with subsequent disease prevalence. Accordingly, the two following two chapters monitor bleaching stress at replicate subtropical locations between 2004-2007 and evaluate the effects elevated temperatures has on the symbiotic zooxanthellae associated with dominant subtropical coral species.

Over the past two decades, there has been growing concern regarding the increasing occurrence and severity of bleaching episodes, which have resulted in the loss of many coral reefs throughout the world (Glynn 1984; Williams and Bunkley-Williams 1990; Hoegh-Guldberg 1995; Brown 1997; Baird and Marshall 1998; Hoegh-Guldberg 1999; Marshall and Baird 2000; Loya *et al.* 2001; Berkelmans *et al.* 2004). Coral bleaching has been described as the dissociation of the symbiotic relationship between zooxanthellae and their mutualistic cnidarian hosts and/or a reduction in photosynthetic pigment concentration as a result of stress (Glynn 1993; Glynn 1996; Brown 1997; Lesser 1997; Hoegh-Guldberg 1999). Stress may result from a number of factors including: changes in salinity (Coles and Jokiel 1978; Hoegh-Guldberg and Smith 1989; van Woesik *et al.* 1995); solar radiation (including ultraviolet radiation) (Hoegh-Guldberg and Smith 1989; Gleason and Wellington 1993; Brown *et al.* 1994; Shick *et al.* 1996; Lesser 1997; 2000; Anderson *et al.* 2001; Fitt *et al.* 2001); pollution (Jones *et al.* 1999): change in seawater temperature (Glynn 1993; Hoegh-Guldberg and Salvat 1995; Glynn 1996; Brown 1997; Lesser 1997; Hoegh-Guldberg 1999; Edwards *et al.* 2001; Fitt *et al.* 2001); or disease (Kushmaro *et al.* 1998; Toren *et al.* 1998; Ben-Haim

et al. 1999; Banin *et al.* 2000; Rosenberg and Ben-Haim 2002; Cervino *et al.* 2004). Moreover, the combined effect of increased seawater temperature coinciding with recent strong El Niño-Southern Oscillation (ENSO) events and periods of high light intensity has caused unprecedented bleaching episodes on a global scale. There is increasing concern that, with seawater temperature expected to rise, mass bleaching events will continue, which may result in the loss of many ecologically and economically important habitats (Hoegh-Guldberg 1999; Wilkinson 1999).

Scleractinian corals have an upper thermal threshold and when this is exceeded, bleaching will occur. This threshold varies over geographical and seasonal scales according to adaptation (over thousands of years) and acclimation (seasonal changes) responses to local yearly maximum and seasonal temperature trends. For example, Berkelmans and Willis (1999) indicated that winter bleaching occurred at temperature 1-2°C below summer thermal maximum values, which may reflect differential temperature susceptibility according to previous short- and long-term temperature history. The global bleaching monitoring program developed by the National Oceanic and Atmospheric Administration (NOAA) utilises bleaching threshold 1°C above average long-term maximum summer monthly temperature to predict mass bleaching and potential coral mortality events (Toscano *et al.* 2000; Strong *et al.* 2004; Lui *et al.* 2006). National Oceanic and Atmospheric Administration coral "hotspot" mapping thresholds are based on 50-km resolution twice weekly night time derived Advanced Very High Resolution Radiometer (AVHRR) sea surface temperature (SST) data and mean monthly maximum (MMM) climatology (Strong *et al.* 2004). Coral bleaching hotspot anomalies (available at www.coralreefwatch.noaa.gov) are determined by calculating the difference between current SST and MMM climatology, which are displayed using a coral thermal index known as Degree Heating Weeks (DHW). Degree Heating Weeks accumulate for a specific oceanic region when SST exceeds the MMM by 1°C, with cumulative weekly periods exceeding MMM indicated on the SST anomaly charts. The DHW product represents the accumulation of above average weekly temperature during the previous 12 weeks. Coral bleaching is expected when four DHW (i.e. four weeks of 1°C - or two week of 2°C above MMM) is exceeded and extensive coral mortality predicted when values are at or above eight DHW. Toscano *et al.* (2000) indicated that finer scale 9-km resolution climatology more accurately reflected field SST during the 1998 mass bleaching event, concluding that higher

resolution hotspot maps predict bleaching in areas missed by the data at 50-km resolution. However, near real time maps that utilise 9-km SST climatology are not available due to the high level of calibration and complex algorithms required; thus the authors concluded that the larger-scale mapping is an appropriate tool for real-time bleaching forecasting.

Mass bleaching events that occurred during summers of 1998 and 2002 throughout the Great Barrier Reef (GBR) were accurately predicted by the NOAA satellite SST anomaly monitoring tool. However, extensive bleaching during early summer 2005-2006 in the southern GBR was not predicted by this bleaching threshold model. As indicated by Weeks *et al.* (2008), NOAA low resolution SST and MMM thermal indices don't take into account seasonal temperature anomalies and therefore do not predict bleaching events when SST is lower than calculated MMM. They further suggested that 4-km climatology and seasonally adjusted thermal thresholds would enable more accurate forecasting of future bleaching events.

Recent studies on the impacts of coral bleaching episodes have mainly been limited to tropical regions (23.5°N to 23.5°S) including the GBR and northern hemisphere localities. The effects of bleaching episodes on recruitment (Gleason 1996; Wilson 1996; Normille 2000; Loya *et al.* 2001), fertilisation (Omori *et al.* 2001), mortality and recovery of corals (Harriott 1985; Quinn and Kojis 1999; Edwards *et al.* 2001; Guzman and Cortes 2001; Suefuji and van Woesik 2001) have been examined in tropical regions. Publications with reference to bleaching events at higher latitudes in southern hemisphere regions are limited. Cellier and Schleyer (2002) quantitatively evaluated the level of bleaching associated with increased seawater temperature and clear water on reefs of South Africa. Patchy bleaching was observed in scleractinian and alcyonacean corals during 2000, when average monthly temperatures ranged between 27.5°C and 28.8°C. When they compared bleaching occurrence and seawater temperature between 1998 and 2000 events, they concluded that increased water clarity and radiation acting synergistically with elevated temperature stress contributed to the higher level of bleaching during summer 2000 compared to summer 1998 event.

Coinciding with the higher than normal SST anomaly during the 1997-98 ENSO event, increased levels of bleaching were observed at high latitude reefs along the east coast of Australia. Increased levels of bleaching were reported from subtropical regions, including the Lord Howe Island Marine Park (LHIMP) located adjacent to the World Heritage listed Lord Howe Island and throughout the Solitary Islands Marine Park (SIMP), northern New South Wales (NSW). Quantitative surveys conducted at LHIMP four months after initial bleaching found that many dominant coral species, including *Isopora cuneata* (previously reported as *Acropora palifera*)*, Pocillopora damicornis, Porites* spp. and *Stylophora pistillata* were recovering from severe bleaching (Kitchener 1998). Additionally, during surveys conducted in the SIMP in summer 1998, many corals from the families Acroporiidae, Pocilloporidae and Dendrophylliidae were observed with a noticeable reduction in symbiotic algae pigmentation (Edgar *et al.* 2003).

Northern NSW subtropical marine communities that are dominated by hard corals are extremely complex biomes with many biotic, abiotic and anthropogenic factors acting in synergy, shaping the structure and function of these unique habitats (Harriott *et al.* 1999). It is important to understand natural variations in community structure and how acute/chronic disturbances affect epibenthic organisms. Long-term monitoring programs are essential in order to understand the complexity and consequences of coral bleaching in response to predicted rise in seawater temperature, especially if bleaching events become more frequent and severe in the future. Therefore, the objective of this study was to examine the relationship between seawater temperature and the spatial and temporal patterns of bleaching within the coral communities in the SIMP and LHIMP, in order to: i) determine whether NOAA SST hotspot charts are a good predictor of potential severe bleaching events at these locations; ii) monitor seasonal variation in bleaching patterns; iii) determine the variability of bleaching susceptibility in subtropical coral species; and iv) predict coral bleaching threshold at 30°S and 31.5°S extrapolated from published bleaching threshold data from northern locations and *in situ* bleaching data collected during this study.

5.3 Methods

5.3.1 Study sites

The SIMP (30°S, 153°E); located on the east coast of northern NSW, and LHIMP (31.5°S, 159°E) which lies approximately 600 km east of mainland Australia have previously been recognised for their high scleractinian coral cover (Veron *et al.* 1974; Veron and Done 1979; Harriott *et al.* 1994, 1995, 1999; Woodroffe *et al.* 2006). Reefs adjacent to four islands within the SIMP and four sheltered and two exposed sites at LHIMP were randomly selected to monitor coral bleaching dynamics between 2004 and 2007 (refer to Chapter 3 for location figures and site descriptions). *In situ* seawater temperature data has been collected from the monitored island sites within the SIMP since 2000.

5.3.2 Seawater temperature

Hastings Tidbit Stowaway temperature loggers were previously deployed at several locations within the SIMP at a depth of 10 m during 2000-2001; unfortunately, similar devices have not been installed at LHIMP. Seawater temperature data was recorded at 30-minute intervals and stored in the loggers for up to 1.5 years. The loggers were removed and temperature data downloaded before being re-calibrated and replaced at each site (H. Malcolm personal communication). Descriptive analysis was performed on the average daily temperatures and results compared between years. Additionally, 50 and 4 km-resolution AVHRR Pathfinder night-time-derived climatology were downloaded from podaac.jpl.nasa.com using the NOAA HDFview Version 2.4 software. These dataset provided continuous SST time series (2001-2008) for the areas of interest. Average weekly climatology from 2001-2008 for both AVHRR products were generated and these datasets were compared with corresponding *in situ* data from the SIMP using Pearson's correlations. If these datasets aligned well with the *in situ* temperature then, monitoring coral bleaching climatology using current NOAA hotspots and DHW bleaching predictors via Coral Reef Check web address would be appropriate for eastern Australia subtropical regions.

Complete long term SIMP and LHIMP SST datasets from 1990-2008 were acquired from the Coral Reef Watch web address. Twice-weekly NOAA AVHRR pathfinder night-time-derived 50-km resolution SST data were used to generate time series plots at

both SIMP and LHIMP locations. In order to determine the rate of increase in average SST at both locations a goodness-of-fit curve was applied to the datasets. This procedure determined the level of SST rise between 1990 and 2008 at 30°S and 31.5°S.

5.3.3 Coral bleaching response

Coral bleaching assessments were completed in conjunction with Australian subtropical white syndrome (ASWS) evaluations within the SIMP (2004 to 2007 summer/winter biannual surveys) and at LHIMP in 2005. Sites selection (including location map: Fig. 3.1) and belt transect survey methodology are described in Chapter 3. Bleaching surveys conducted within the SIMP were completed during March and August, which corresponded to the warmest and coolest months, respectively. Sampling at LHIMP was completed during May, when seawater temperature ranged between 21-22°C.

During belt transect coral stress evaluation surveys, individual corals were recorded as bleached according to pigmentation colour characteristics. Prior to stress assessment dives, all coral species observed at the study sites were compared to the Coral Health Monitoring Chart (CHMC, Siebeck *et al.* 2006) and normal pigment colour was calibrated with the colour chart codes. These codes were used as a reference during all subsequent coral stress survey dives. If a colony displayed white, patchy white or pale colouration relative to normal pigmentation of that coral species at that location, then the individual coral was recorded as either moderately (1-50% tissue bleaching) or severely (51-100% tissue bleaching) bleached (consistent with Marshall and Baird 2000; McClanahan *et al.* 2004) according to either the percentage of colony discolouration and/or the level of pigment paling (refer to Fig. 3.2d for examples). For example, if an individual colony from a coral species that normally displayed a pigmentation colour similar to the monitoring chart C6 code had a colouration characteristic of either C4 or C5, this colony would be recorded as moderately bleached. In contrast, if a colony of the same species displayed a pigment colouration lighter than C4, then the severely bleached category was recorded. Additionally, if a region of less than 50% of the colony surface area was completely bleached (i.e. white, tip bleaching), the moderately bleached category applied.

5.3.4 Statistical analysis

5.3.4.1 Coral bleaching response

Prior to analyses the proportion of each bleaching category (number of colonies within each bleaching category divided by the total number of corals within each transect) were calculated for all coral taxa. A single scaled measure, bleaching susceptibility index (BSI), was calculated for total coral and coral family from each replicate transect bleaching response data using a modification of the bleaching index formula given in McClanahan (2004); only three categories were utilised in the study, because mortality associated with bleaching could not be accurately quantified. Bleaching susceptibility index was calculated using the formula:

$$BSI = (0un + 1mb + 2sb) / 2$$

where proportional data from unbleached (un), moderately bleached (mb) and severely (sb) bleached categories were utilised. This formula appropriately weighted each category to account for increased stress resulting from greater pigmentation loss.

Spatial and temporal patterns of BSI within the SIMP coral community were analysed using a factorial ANOVA with Minitab statistical package. During the survey period seawater temperature within the SIMP did not exceed bleaching thermal thresholds and extensive bleaching of the coral community did not occur, thus year was treated as a blocking factor, season and location considered fixed factors and site was nested within location. Prior to analysis, BSI data were tested for normality and homogeneity of variance and, where necessary, root arc-sin transformed.

In order to understand the difference in coral family bleaching susceptibility, family BSI data from the SIMP summer surveys and BSI data from LHIMP study were analysed using a three-factor (year blocked, location fixed factors and family random) and a two-factor (sites and family were random factors) ANOVA, respectively. Student-Newman Keuls (SNK) tests were performed on each dataset to explore further differences between families within sites and within families between sites.

5.3.4.2 Predicting subtropical bleaching thermal threshold

Linear and second-order polynomial regression models (Graphpad Prism v 5.0) were fitted to reported thermal threshold data from tropical and other subtropical locations (Hoegh-Guldberg 1999; Celliers and Schleyer 2002). Comparing these models indicated that the quadratic model was a better fit of the data and was therefore used to extrapolate a theoretical bleaching threshold for SIMP and LHIMP coral communities. This index was then compared to *in situ* and SST datasets to propose a coral bleaching threshold hypothesis for the eastern Australian subtropical region and estimate a minimum period of exposure to thermal stress required to induce a thermal bleaching response in subtropical coral communities.

5.4 Results

5.4.1 Seawater temperature

In situ seawater temperature recorded between 2001 and 2008 tended to be highly variable over small temporal and spatial scales (Fig. 5.1a). Seawater temperature data at NSI was generally higher than the midshelf island reefs (NWSI and SWSI), and this pattern was consistent throughout all seasons and years (Fig.5.1a, b). Average daily maximum temperature was highest at NSI and ranged between 24.99 and 27.35°C (Table 5.1). Maximum daily temperature was lowest during all years at SWSI, ranging between 24.32 and 25.94°C (Table 5.1). The temperature logger at the more southern location (SWSI) was installed at a later date than the other two locations and, during 2004-2005, the temperature logger was lost from the substratum; hence an incomplete temperature dataset shown in Figure 5.1a.

Seasonal patterns of temperature variation are evident with temperature rising to as high as 27°C during summer and falling to below 17°C during winter within the SIMP (Fig. 5.1a, b). Weekly temperature fluctuations of up to 5°C occur consistently at the midshelf island reefs, with an 8.4°C differential observed at SWSI during a one-week period (Fig. 5.1a; 31/01/2008-07/02/2008). Daily temperature changes up to 4°C day^{-1} were common at all locations particularly during summer months. Average seawater temperature was consistently 1-2°C higher at NSI compared to the other locations (Fig. 5.1b). Average seawater temperatures at NWSI and SWSI were similar throughout the

years with some small differences during summer periods noted (Fig. 5.1b). Summer seawater temperatures were highest during 2006 at all locations, and average daily temperature exceeded 27°C on three occasions at NSI. However, the number of days seawater temperature exceeded 25°C was greatest during 2002, where 52, 27 and 33 days exceeded this measure at NSI, NWSI and SWSI, repetitively (Table 5.1). Maximum monthly mean temperatures consistently occurred during February and March during most years at all island locations (Table 5.1). At NSI this measure was highest in 2006, but was highest in during February 2002 at the midshelf islands.

Sea surface temperature data shows weekly, seasonal and yearly differences in temperature at subtropical Australian reefs between 1990 and 2008 (Fig. 5.1c). Maximum weekly SST recorded during this time occurred in 1998, with similar values recorded in 1996 and again in 2006. Prior to 1996, maximum weekly SST within the SIMP did not exceed 26.5°C; however, nine out of the next 13 years recorded maximum weekly temperatures > 26.5°C (Fig. 5.1c). Temperatures at LHIMP tended to be lower than the SIMP with average SST not exceeding 26°C during this period. However, MMM values recorded at LHIMP tended to be of similar magnitude to those recorded at SWSI (Table 5.1). Linear regression analysis of sea surface temperature using average yearly SST data, showed that there was a significant rise in SST between 1990 and 2008 at both locations (SIMP $F_{1,17} = 4.78$, $p = 0.044$, LHIMP $F_{1,17} = 5.84$, $p = 0.028$), but these models (SIMP°C = 0.027*(year) – 31.43, LHIMP°C = 0.034*(year) – 46.67) only explained 23 and 26% of the variation between the two variables in the SIMP and LHIMP data sets, respectively. However, removing 1998 data, which was an outlier in the data sets, showed a stronger relationship (40 and 36% for SIMP and LHIMP, respectively). During this period, average SST within the SIMP and LHIMP increased by 0.029 and 0.034°C $year^{-1}$, respectively.

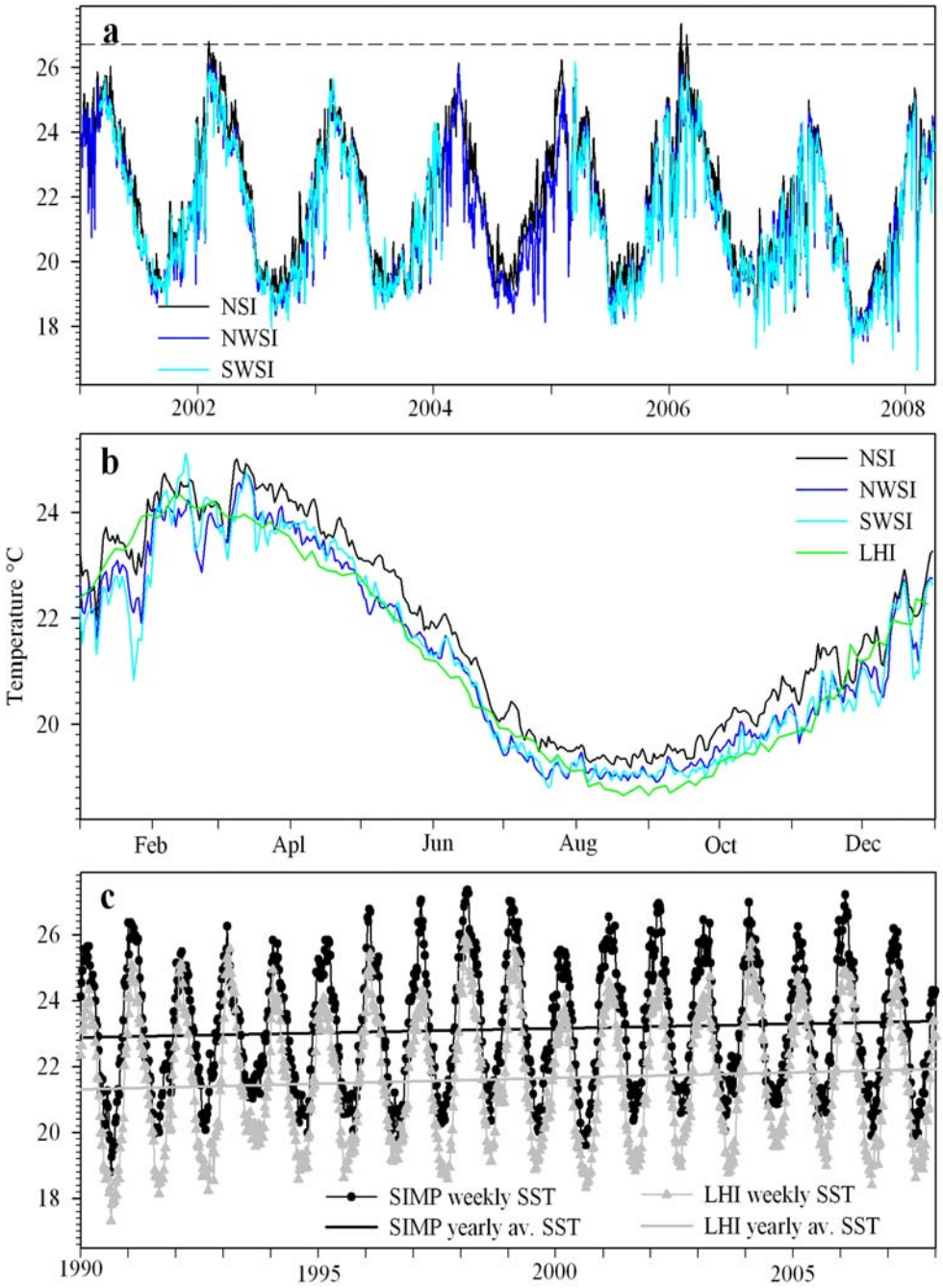

Figure 5.1: SIMP and LHIMP seawater temperature data: a) mean daily *in situ* temperature data collected at three island locations between 2001 and 2008: North Solitary Island (NSI); North West Solitary Island (NWSI); and South West Solitary Island (SWSI). Dotted line indicates hypothesised subtropical bleaching threshold; b) average seasonal pattern of seawater temperature at three SIMP island locations and average yearly SST from LHIMP; and c) mean weekly SIMP and LHIMP sea surface data acquired from NOAA climatology (podaac.jpl.nasa.com). Solid line indicates rate of average temperature rise at both location.

Table 5.1: Summary of *in situ* seawater temperature data collected from reefs adjacent to three islands in the SIMP, North Solitary Island (NSI), North West Solitary Island (NWSI) and South West Solitary Island (SWSI). LHIMP SST data acquired from NOAA climatology (podaac.jpl.nasa.com) are shown in the absence of LHIMP *in situ* temperature data. DNC = data not complete

		Year						
Location	**Variable**	**2001**	**2002**	**2003**	**2004**	**2005**	**2006**	**2007**
SIMP								
NSI	Av. daily max.	26.05°C	26.80°C	25.65°C	26.14°C	26.23°C	27.35°C	24.99°C
	Av. daily min.	18.95°C	18.73°C	18.78°C	18.87°C	18.38°C	18.14°C	17.61°C
	MMM	25.13°C	26.07°C	24.30°C	25.07°C	24.06°C	26.10°C	23.40°C
	Warmest month	(Mar)	(Feb)	(Feb)	(Mar)	(Apr)	(Feb)	(Mar)
	N° days > 25°C	34	52	4	19	28	37	0
	N° days > 26°C	1	18	0	1	4	17	0
	N° days > 26.6°C	0	3	0	0	0	6	0
NWSI	Av. daily max.	25.57°C	26.16°C	25.34°C	26.03°C	25.82°C	26.00°C	24.65°C
	Av. daily min.	18.67°C	18.27°C	18.76°C	18.13°C	18.09°C	17.99°C	16.91°C
	MMM	24.82°C	25.55°C	24.08°C	24.93°C	23.49°C	24.65°C	22.94°C
	Warmest month	(Mar)	(Feb)	(Feb)	(Mar)	(Apr)	(Feb)	(Mar)
	N° days > 25°C	16	27	9	12	10	14	0
	N° days > 26°C	0	2	0	1	0	1	0
	N° days > 26.6°C	0	0	0	0	0	0	0
SWSI	Av. daily max.	DNC	25.94°C	25.67°C	DNC	DNC	25.79°C	24.32°C
	Av. daily min.	DNC	17.96°C	18.53°C	DNC	DNC	17.33°C	16.83°C
	MMM	24.90°C	25.39°C	24.39°C	DNC	23.36°C	24.60°C	22.97°C
	Warmest month	(Mar)	(Feb)	(Feb)		(Mar)	(Feb)	(Apr)
	N° days > 25°C	DNC	33	13	DNC	DNC	17	0
	N° days > 26°C	DNC	0	0	DNC	DNC	0	0
	N° days > 26.6°C	DNC	0	0	DNC	DNC	0	0
LHIMP								
	Av. daily max.	24.3	24.7	24.4	25.2	24.5	25.2	24.4
	Av. daily min.	18.0	18.2	18.4	18.7	18.6	18.4	18.6
	MMM	23.67°C	23.89°C	24.00°C	24.85°C	24.21°C	24.65°C	23.99°C
	Warmest month	(Mar)	(Feb)	(Feb)	(Feb)	(Mar)	(Feb)	(Mar)

Comparing SST and *in situ* temperature recorded at 10 m within the SIMP showed that 50-km resolution satellite-derived SST data does not accurately predict temperatures at 10 m. Maximum SST between 2001 and 2007 was on average 1.50°C ± 1.25 (SD), 2.01°C ± 1.25 and 2.04°C ± 1.35 higher than *in situ* measures recorded at NSI, NWSI and SWSI, respectively. These discrepancies were confirmed with the concordance analysis which plotted the *in situ* temperature data against the satellite derived SST (Fig. 5.2a). Pearson correlations indicated that 50-km resolution SST measurements were poor predictors of *in situ* seawater temperature. However, the 4-km resolution AVHRR derived climatology data showed a greater concordance with *in situ* data from NSI (Fig 5.2b).

5.4.2 Spatial and temporal patterns of bleaching in the SIMP

A total of 83,951 individual coral colonies were counted at the eight sites investigated between 2004-2007, of which 2,950 and 138 colonies were recorded as moderately and severely bleached, respectively. Total coral bleaching (moderate and severe categories pooled) was higher during the summer survey periods compared to the surveys conducted during cooler months for all years (Fig. 5.3). Total bleaching varied between 4 to 16% in summer and < 2% during winter surveys (data pooled within season to the location level). The highest number of colonies noted as moderately bleached was during summer 2005 (11% pooled from all sites); however severe bleaching was greatest during summer 2006 (< 1% pooled all sites). Total bleaching response was highest at Anemone Bay during summer 2005 where 22% and 1% colonies were observed with moderate and severe bleaching response, respectively. At the other sites, moderate and severe bleaching ranged between 6 and < 1% (SSI-Coral Corner) and 12 and 1% (NSI-Trail Mooring), respectively. Total bleaching response during summer surveys was highest at NSI compared to the more southern nearshore island reefs (Fig. 5.3).

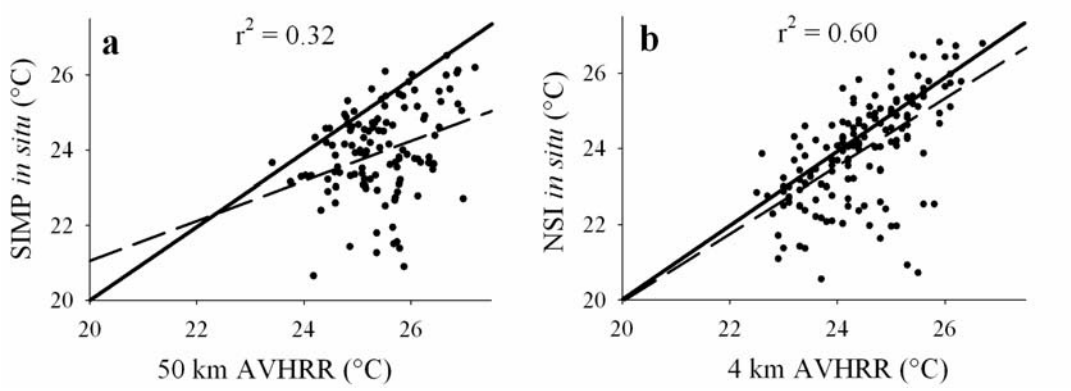

Figure 5.2: Correlations between: a) average weekly summer seawater temperature derived from *in situ* loggers and satellite 50-km resolution SST recorded between 2001 and 2008; and b) weekly *in situ* temperatures recorded during summer at North Solitary Island (NSI) compared to 4-km resolution AVHRR climatology recorded adjacent to NSI. Dashed lines indicate the *in situ* temperature versus the SST line of best fit. A perfect correlation is indicated by the solid line which is 45° to the X and Y axes.

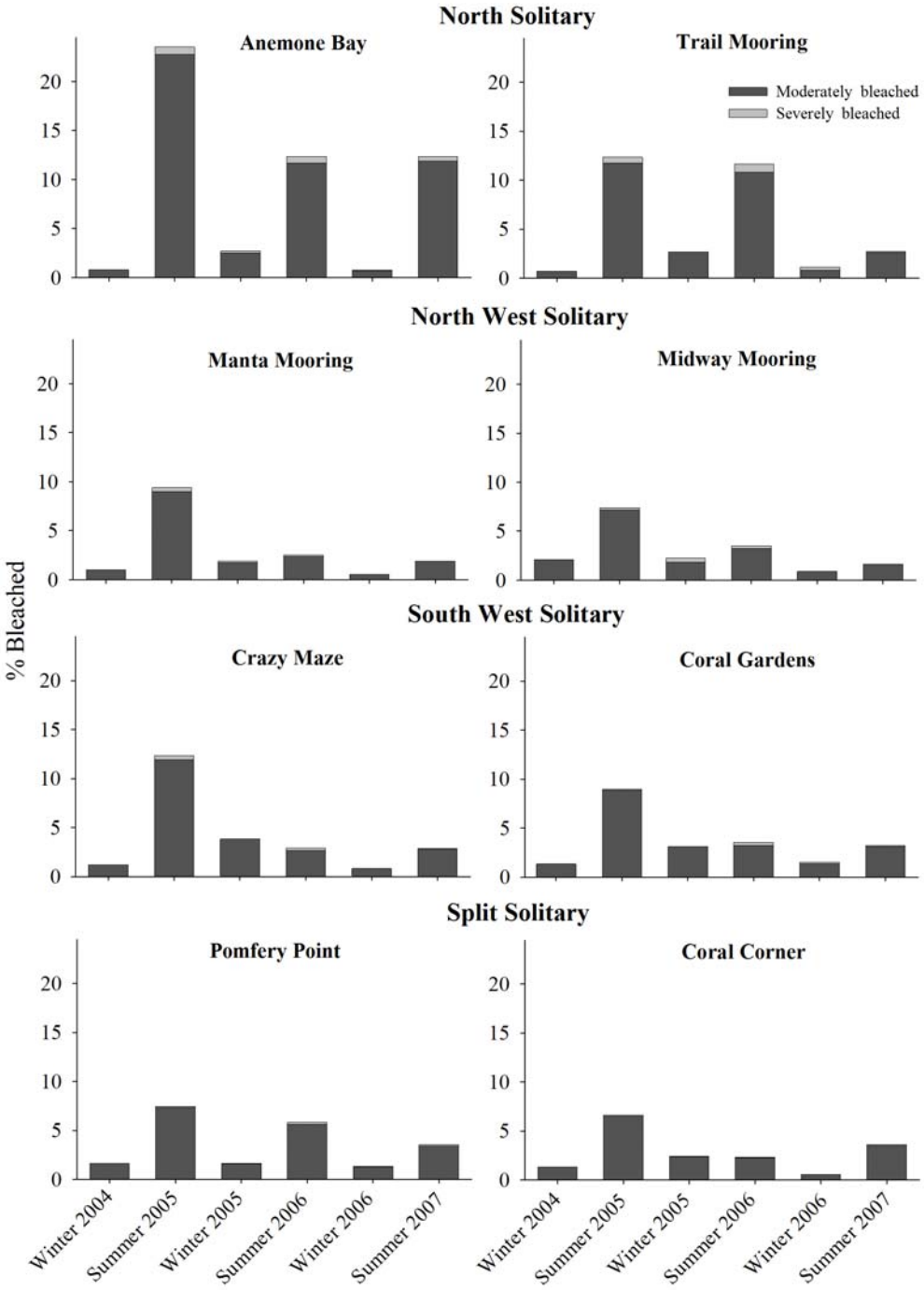

Figure 5.3: Average proportion (n = 5 belt transect per site) of moderate and severe coral bleaching categories recorded at eight island reefs within the SIMP surveyed biannually between 2004 and 2007

5.4.3 Spatial and temporal patterns of bleaching susceptibility in the SIMP

Total BSI was significantly higher during summer survey periods compared to cooler periods ($F_{1,8} = 65.0$, $p = 0.0013$) and there was a general trend for total BSI to be higher at all sites during summer 2005 compared to other summer survey periods. This was confirmed by the SNK analysis, which indicated that total bleaching response was significantly higher during summer 2005 compared to the previous and following summers ($p < 0.05$). In contrast, total BSI was significantly higher during winter surveys in 2006 than the other winter periods ($p < 0.05$).

During this study, bleaching response was significantly more variable at the smaller spatial scale (Sites within location: $F_{4,192} = 5.5$, $p = 0.0003$) than between locations ($F_{3,192} = 4.24$, $p = 0.0787$). However, SNK contrasts showed that within location differences were only significant during summer 2005 and 2007 at NSI and at SSI in 2006. All other within location planned contrasts (21 out of 24) were not significantly different ($p > 0.05$).

5.4.4 Coral family bleaching susceptibility in the SIMP

Five coral families (Acroporidae, Dendrophylliidae, Faviidae, Pocilloporidae and Poritidae) were observed with variable levels of pigmentation loss during this study. Common coral species from the families Agariciidae, Mussidae and Siderastereidae, showed no loss of pigmentation during this time. The mean proportion of total bleaching response was variable at the family, year, season and location levels (Fig. 5.4). Pocilloporidae spp., notably *Pocillopora damicornis* and *Stylophora pistillata*, were frequently observed with tissue paling, particularly at the branch tips during summer surveys at all island sites. Total bleaching response (moderate and severe combined) was highest in this taxon during the 2005 summer surveys, during which time total bleaching ranged between 22.5 ± 3.1% (NSI) and 34.6 ± 5.8% (NWSI). Poritidae colonies were also regularly observed with decreased tissue colour at all locations, particularly at NSI, where bleaching reached 44.2 ± 8.2% in 2005 (Fig. 5.4). The majority of total bleaching was in the moderate category during all survey periods; however, during the 2006 summer survey, the mean proportion of severe bleaching in the dendrophyllids reached 15.0 ± 10.7% at NSI. During this period, only 10 individual colonies were counted in the belt transects at NSI, with only two individual colonies

severely bleaching during this time (Fig 5.4). Bleaching response in this taxon also increased during summer at NSWI, SWSI and SSI, approaching 5% (Fig. 5.4).

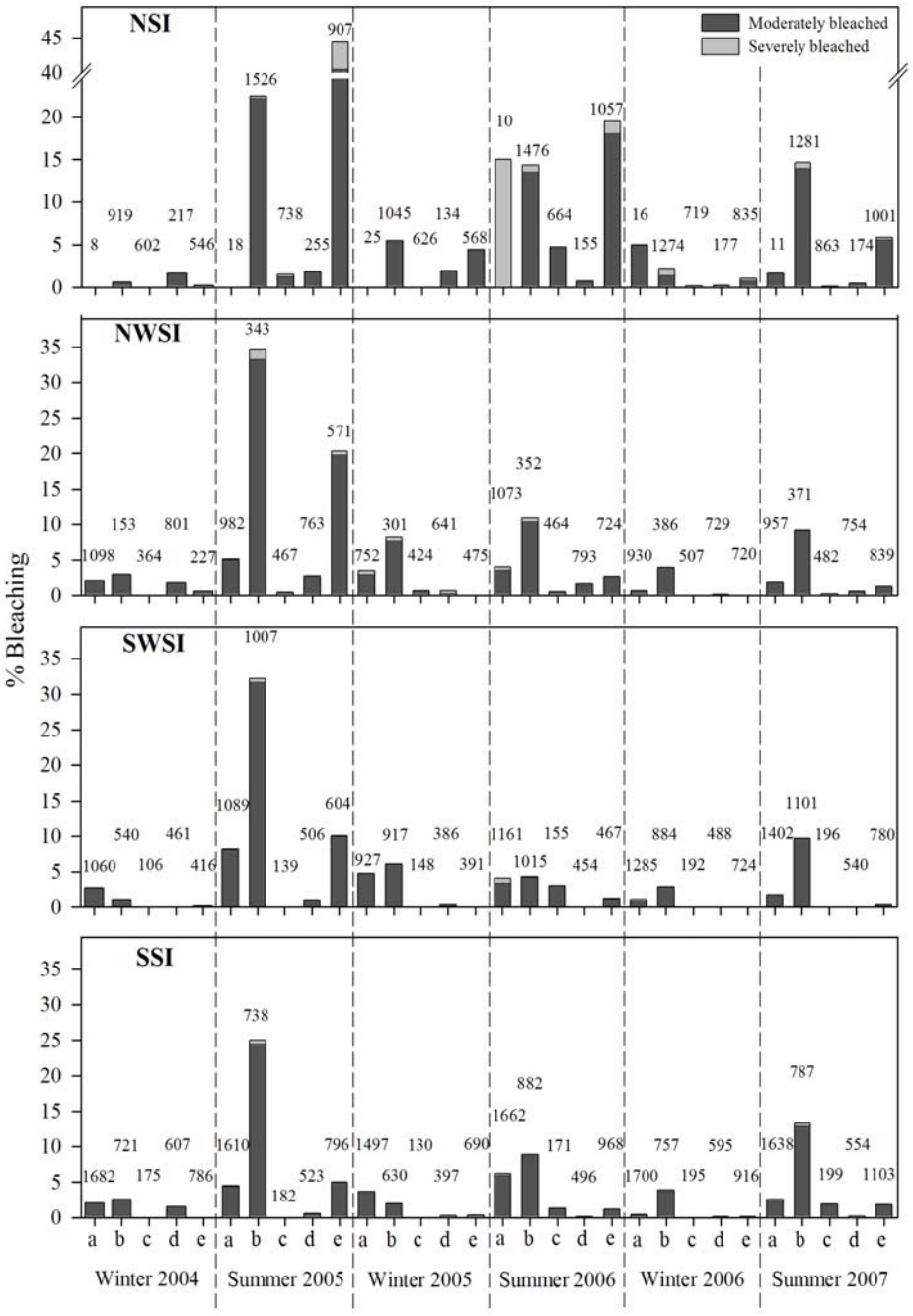

Figure 5.4: Average proportion of bleaching response (moderate and severe) recorded for different families during bleaching surveys at four island locations within the SIMP. a) Dendrophylliidae b) Pocilloporidae c) Acroporidae d) Faviidae and e) Poritidae. Numbers above bars indicate total colonies counted within each family at each location during summer and winter surveys.

Family differences in bleaching susceptibly are apparent with an overall significant difference in BSI ($F_{4,24}$ = 281.1, p <0.001). There was no significant location effect, although there was a significant location by family interaction ($F_{8,24}$ = 26.05, p < 0.001), indicating that patterns of family bleaching susceptibility were variable across all locations. Planned contrasts (SNKs), which tested for differences in coral family bleaching susceptibility within location, showed that Poritids and Pocilloporids were significantly more susceptible at NSI, whereas the BSI for Pocilloporids was significantly higher at all other locations (p < 0.05), with Dendrophyllids more susceptible than Poritids, Acroporids and Faviids at the southern locations.

5.4.5 Spatial patterns of bleaching in the LHIMP

A total of 7042 individual colonies from eleven scleractinian families were recorded at the six sites evaluated, of which 396 (5.74%) were observed with varying degree of pigmentation loss. The mean proportion of moderate bleaching was an order of magnitude higher than the mean proportion for severe bleaching. The total proportion of bleached colonies ranged between 4.68% at Comet's Hole and 6.36% at Erscott's Hole. Overall, five hard coral families (Acroporidae, Dendrophylliidae, Faviidae, Pocilloporidae, and Poritidae) were observed with reduced pigmentation (Fig. 5.5). Bleaching was present in acroporids at all sites and ranged between 0.61 and 15.13%. Additionally, poritids and pocilloporids were observed with varying degrees of pigmentation loss at all sites. The highest bleaching response was within the pocilloporids at the exposed Malabar Reef, where 12.77 and 3.22% of this population were moderately and severely bleached, respectively. Interestingly, faviids were only bleached at Noddy Island and Malabar Reef (exposed sites) and dendropyllids were only bleached at Noddy Island (Fig. 5.5). No dendropyllids were recorded within the lagoon sites and only 9 and 39 colonies were counted at Malabar Reef and Noddy Island, respectively.

5.4.6 Coral family bleaching susceptibility in the LHIMP

Patterns of family bleaching response tended to be similar to those observed within the SIMP, with pocilloporids and poritids consistently recorded as bleached, although the level of bleaching response in Acroporids tended to be higher at LHIMP (Fig. 5.5). Statistical analysis of BSI was only performed on the families that recorded bleaching at

all sites. This resulted in dendrophyllid and faviid data from the exposed sites being omitted from the analysis.

Results from the two-way ANOVA indicated that there was no significant difference in BSI between sites and between families, but there was a significant interaction between these factors ($F_{6,54} = 3.0$, $p = 0.0045$). Bleaching susceptibility index for Pocilloporidae was higher than for acroporids and for poritids at the two exposed sites but only significantly different at Malabar Reef ($p < 0.05$). In contrast, BSI for Acroporids, notably *Isopora cuneata* and *Montipora* spp. was highest at North Bay Wreck and Comet's Hole, but this was not significantly higher than other families at these sites.

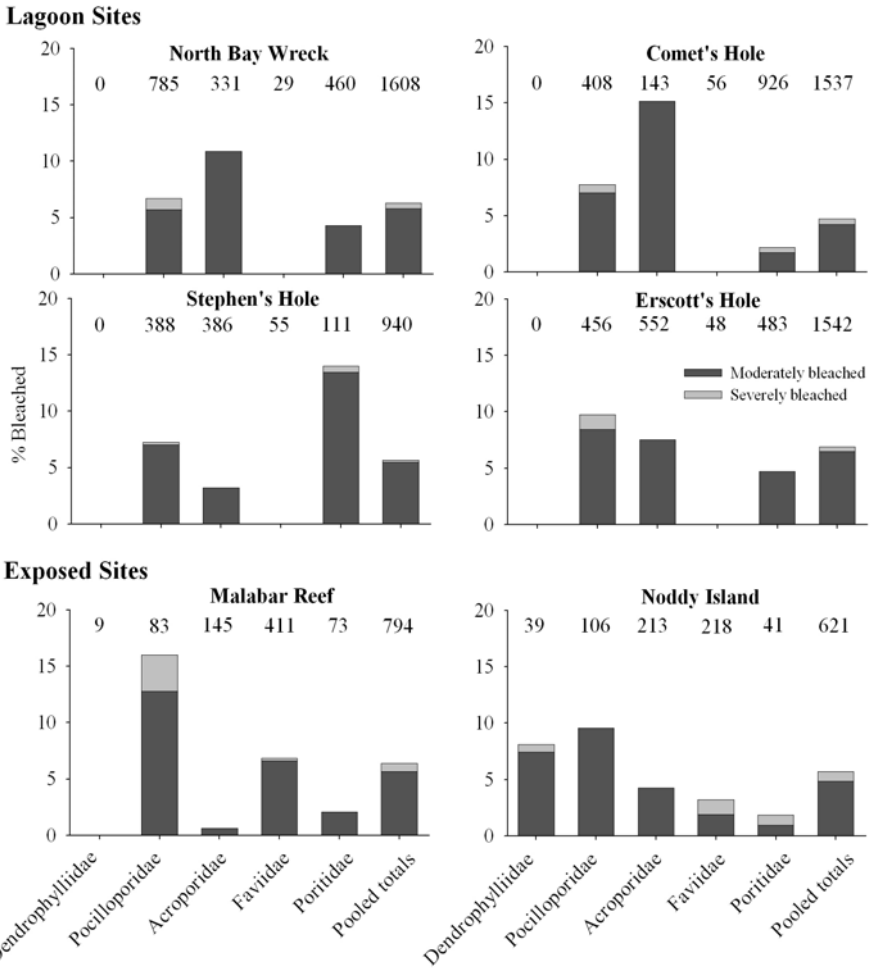

Figure 5.5: Average proportion of bleaching response (moderate and severe) for different families at reefs adjacent to Lord Howe Island recorded in May 2005. Numbers above bars indicate total colonies counted within each family at each site.

Different species of poritids displayed variable bleaching susceptibility. For example, many *Porites heronensis* bleached at most sites particularly at Stephen's Holes, whereas no *P. lutea* and *P. lichen* colonies displayed any decrease in pigmentation. For the pocilloporids, differences were also apparent during this study, with bleached *Stylophora pistillata* colonies observed at the exposed site; however, no bleaching was noted in *Pocillopora damicornis* corals. Patterns of bleaching susceptibility were not consistent between sites because different coral species were found at different sites; therefore, it is difficult to determine any site effect because there was in adequate representation of each susceptible taxon at the sites. Thus the ability to formulate testable hypotheses with these data is limited.

5.4.7 Subtropical bleaching thermal threshold

Thermal bleaching threshold values reported in the literature displays a distinct inverse trend with latitude (Fig. 5.6). Results from the second-order polynomial analysis indicated a significant relationship ($F_{2,7} = 175.70$, $p < 0.0001$) between these variables; the model accounted for a high proportion of the variance in the data set (Fig. 5.6, $r^2 = 0.99$). Applying the equation generated by the regression procedure indicated that the hypothetical thermal bleaching threshold for corals located at 30° (SIMP) and 31.5°S (LHIMP) extrapolated from other published thresholds are 26.66 and 26.51°C, respectively. The hypothetical bleaching threshold for the SIMP has previously been exceeded in 2002 and 2006, where average *in situ* daily seawater temperature at NSI exceeded this measure 3 and 6 times, respectively. However, this temperature has not been exceeded at 10 m at the midshelf islands (Table 5.1). As indicated by the weekly SST data (Fig. 5.1c), average weekly SST at 30°S has exceeded this measure during seven years since 1995. However, the hypothetical bleaching threshold for LHIMP has not been exceeded during the past 18 years (Fig. 5.1c).

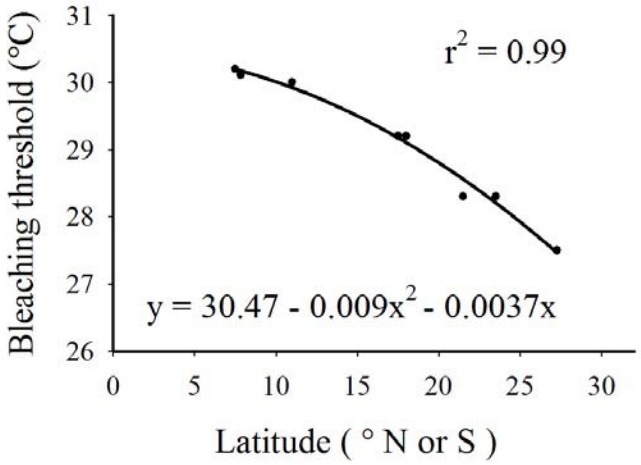

Figure 5.6: Second-order polynomial plot of thermal bleaching threshold derived from reported thermal threshold estimates reported in Hoegh-Guldberg (1999) and Cellier & Schleyer (2002). Bleaching thermal stress values for regions outside these latitudes may be hypothetically extrapolated using this regression equation.

5.5 Discussion

Monitoring the bleaching response of corals on SIMP and LHIMP reefs between 2004 and 2007 showed that severe bleaching did not occur, but there was evidence of seasonal patterns of bleaching and differential family susceptibilities. Additionally, SST anomaly tools used to monitor bleaching do not adequately predict *in situ* temperatures in the SIMP with greater concordance shown with higher resolution satellite data (i.e. at the 4-km resolution).

During this study, a severe bleaching event was reported throughout the southern GBR (2005-2006), but increased bleaching response was not reported south of 25.5°S latitude along the east coast of Australia. During this episode, a large pocket of warm water (2°C above early summer MMM) lay along the southern GBR coast for several months (approx. 20-24°S, Weeks *et al.* 2008). Fortunately, during this time, northward-flowing cooler water and mixing of deep upwelled water restricted the movement of this warm water body south of Fraser Island, Queensland (approx. 25°S). *In situ* seawater temperature within the SIMP during this period only exceeded 27°C on three occasions at NSI, (Feb 5th,6th and 22nd).

5.5.1 Predicting subtropical bleaching events using satellite derived SST

Results from this study suggest that monitoring bleaching indices using satellite-derived climatology may over estimate bleaching events on subtropical eastern Australia reefs. Hotspot and DHW thermal imagery utilises 50-km resolution satellite-derived SST and, as shown here, this resolution does not correlate well with temperature measured *in situ*. However, finer scale, 4-km resolution SST gives a better representation of *in situ* temperatures.

Seawater temperature within the SIMP is dynamic and varies at small spatial and temporal scales due to the effects of the East Australian Current (EAC), longshore drift and upwelled waters. Depending on wind speed and direction, oceanic water movement supplies either warm, nutrient poor waters from the Coral Sea or cooler nutrient rich southern waters to this location. Water temperature can be 2-3°C cooler at 10 m compared to the sea surface due to established thermoclines (personal observations). McClanahan *et al.* (2004) indicated that satellite-derived temperature data correlated well with *in situ* temperature data that is pooled over large temporal and spatial scales, but there are problems in predicting nearshore bleaching response to temperature due to land-mass interference. Additionally, as shown here, seawater temperature can vary between 1 – 2°C between offshore and nearshore reefs and, with approximately 6 km between island sites, the 50-km resolution would be averaging temperatures that differed appreciably.

Weeks *et al.* (2008) recently noted that bleaching thresholds of corals varies seasonally and that a single bleaching threshold index (1°C above MMM) and low spatial resolution data derived from satellite warning systems, do not predict severe bleaching events when thermal anomalies occur when maximum seawater temperatures are not predicted (i.e. early summer). They suggested that seasonally-adjusted thermal indices and higher resolution satellite products improve bleaching predictions for nearshore reefs. This is consistent with the finding from this study, which showed a much stronger correlation between *in situ* data and 4-km resolution SST product.

Between 1990 and 2008 there was a significant increase in average yearly SST of 0.029 and 0.034 °C year^{-1} at the SIMP and LHIMP, respectively. These rates of change are higher than those reported at tropical locations over the same time period (reviewed in

Celliers and Schleyer 2002). It has been shown that over the past 20 years the rate of temperature rise has been greatest within the southern GBR compared to central and northern GBR (Hoegh-Guldberg 1999). This suggests that rate of ocean warming is faster at higher latitudes. This rise in seawater temperature may result in ocean temperatures adjacent to northern NSW exceeding the hypothetical 26.6°C bleaching threshold every year by 2030. This is consistent with predictions of annual bleaching events occurring by 2030 throughout the GBR (Hoegh-Guldberg 1999).

5.5.2 Coral family bleaching response

Throughout this study, moderate bleaching (partial and tip bleaching) in a suite of coral species were observed during summer and winter surveys at all sites investigated. Total bleaching susceptibility was greatest at the more northern location within the SIMP, where seawater temperature tended to be higher than the other sites. Many *Porites heronensis* corals were observed with a reduction in pigmentation at NSI during summer surveys. These colonies bleached during mid to late summer with increased pigmentation observed during April when seawater temperatures decrease and photosynthetically active radiation (PAR) intensity declined (unpublished data). This negative response to high summer temperature in the presence of high light may explain why *P. heronensis* is common in subtropical localities but rare in the tropics (Veron 2000b). However, other abiotic and biotic factors need to be considered when explaining distributions patterns. In contrast, the bleaching response in the massive *P. lutea* and *P. lichen* corals observed at LHIMP was low, even within the shallow lagoon sites. Massive *Porites* colonies have previously shown moderate bleaching susceptibility to thermal stress (Marshall and Baird 2000); however, branching poritids have previously displayed significant bleaching response and associated mortality on Kenyan reefs during the 1998 mass bleaching event (McClanahan *et al.* 2004). Assemblage composition may also contribute to the pattern of bleaching susceptibility within the SIMP and LHIMP. During this study, the bleaching susceptibility of dominant corals families was significantly higher than rarer ones. This may indicate that variation in bleaching susceptibility between locations may be associated with temperature and light history as well as ecological factors. Marshall and Baird (2000) indicated that environmental factors (i.e. temperature and light intensity) may explain

large-scale patterns of bleaching occurrence, with small-scale patterns determined by assemblage composition.

Coral communities associated with SIMP midshelf islands regularly experience high turbidity, which decreases PAR and ultraviolet radiation (UVR), both of which contribute to coral bleaching. Suspended sediments and increased levels of phytoplankton can result in a reduction of irradiance and therefore may reduce bleaching response in corals during periods of thermal stress at these locations. Jokiel and Brown (2004) found that corals associated with turbid environments in Hawaii suffered minimal bleaching even though they were exposed to similar temperatures that caused bleaching in clearer waters. They suggested that reduced light penetration may have explained these observations. In contrast, NSI and LHIMP coral communities may be more susceptible to temperature bleaching due to more intense PAR and UVR. Lying further offshore than the other sites, water clarity is consistently greater at NSI - PAR intensity of approximately 200 μmol m^2 s^{-1} higher at 10 m bathometry during summer compared to the midshelf reefs (refer to Chapter 6). Similarly, LHIMP lagoon sites have clear water due to minimal terrigenous runoff, which results in increased PAR and UVR penetration, potentially further damaging the photosystem of the symbiotic zooxanthellae during periods of thermal stress. Further research is required in order to determine the interactions between light intensity and temperature as they relate to bleaching response in subtropical corals.

The bleaching response of pocilloporids, notably *Pocillopora damicornis* and *Stylophora pistillata* was significantly higher than for all other families within the SIMP. However, this was not the case at LHIMP, where the response of this taxon was not statistically higher than other affected families. However, many partial and severe bleached *Stylophora* colonies were observed, particularly at Malabar Reef. These two branching species have shown high bleaching susceptibility when temperatures exceeded 30ºC at other locations including within the GBR (Marshall and Baird 2000; Hueerkamp *et al.* 2001; Vargas-Angel *et al.* 2001; McClanahan *et al.* 2004). Variation in bleaching susceptibility within this taxon between subtropical locations many be due to the large geographical distances and erratic larval connectivity between high latitude eastern Australian reefs. Millar and Ayre (2008) found that there was a clear separation in genetic population structure in *P. damicornis* colonies sampled at LHIMP compared

to corals found in the SIMP. They showed that genetic diversity of *P. damicornis* at LHIMP was more similar to northern GBR populations than colonies at similar latitudes along the east coast of mainland Australia. This genetic similarity may result in a higher thermal threshold of *P. damicornis* LHIMP populations than that of the SIMP populations, which may explain why this species is more susceptible to bleaching within the SIMP than at LHIMP.

Scleractinian corals within the SIMP are exposed to a varied temperature regime throughout the year, with temperatures ranging between 16 and 28°C. This high level of variation may generate evolutionary pressures to develop resilience mechanisms for the coral holobiont, enabling them to adjust to changing temperature within a short period of time. In contrast to coral reefs environments such as the GBR, seawater temperature varies considerably at both small and large time scales along the NSW coastline. Therefore, hard corals within the SIMP require short-term physiological mechanisms that help to prevent thermal stress and damage. Homeostatic processes such as, increased production of mucus polysaccharides which contain microsporine amino acids (MMA) that absorb UVR, endosymbiont reshuffling to more heat or cool tolerant clades if multiple symbionts are associated with subtropical coral species (Chen *et al.* 2005a), and the production of fluorescence pigments (Salih *et al.* 2000), provide acclimation and adaptive mechanisms that increase the ability of the holobiont to combat stress caused by temperature variations.

Differential bleaching susceptibility among taxa may also be attributed to many physiological factors, such as species dominance at different locations, morphological characteristics (i.e. growth form, colony size and tissue thickness) and symbiont type. The numerically dominant pocilloporids and poritids observed within the SIMP and acroporids that dominate the fringing reef of LHIMP, were more susceptible to pigment loss relative to other taxa. These findings are consistent with previous reports of bleaching susceptibility at more northern locations (Marshall and Baird 2000; McClanahan *et al.* 2004). In contrast, *Turbinaria* spp. (Family Dendrophylliidae) have previously been regarded as one of the least susceptible groups to bleaching throughout the GBR (Marshall and Baird 2000). However, at the midshelf island reefs, where this genus dominates, bleached colonies were regularly observed throughout the year, particularity during the warmer months. These results may indicate that if a severe

bleaching event and subsequent bleaching mortality occurred in the future at these locations, loss of a high proportion of the coral cover may occur. This has been observed at other locations where dominant coral species susceptible to thermal bleaching have significantly declined in abundance following mass bleaching episodes (Goreau *et al.* 2000). Acroporids that dominate shallow inner and southern GBR reefs have succumbed to repeated bleaching episodes in recent times. Other branching genera such as *Seriatopora*, S*tylophora* and *Pocillopora* have also succumbed to temperature bleaching stress at other locations. If thermal stress occurs more constantly as predicted, a shift from branching pocilloporid and acroporid-dominated coral communities, to a reef containing larger numbers of sub-massive and encrusting growth forms is predicted at high latitude east Australian reefs.

5.5.3 Subtropical bleaching thermal threshold

By modelling the seawater temperature data and bleaching threshold indices from other locations, the prediction can be made that the summer bleaching threshold within the SIMP and LHIMP are 26.66°C and 26.51°C, respectively. However, as indicated above, this measure does not take into consideration seasonal differences in coral susceptibility to temperature-induced bleaching as well as other variables such as light intensity that are known to cause bleaching in isolation or in combination with other parameters. It is hypothesised that thermally induced bleaching would occur throughout eastern Australia coral populations during periods when seawater temperature exceeds the predicated threshold for a period greater than four weeks. This however, would only occur when the EAC exposes reef communities to higher than normal summer seawater temperatures for extended periods, with minimal mixing of cooler waters.

CHAPTER 6 FLUORESCENCE ANALYSIS TO DETERMINE PHOTOSYNTHETIC EFFICIENCY AND STRESS DUE TO INCREASED TEMPERATURE AND IRRADIANCE

6.1 Abstract

Pulse amplitude modulated (PAM) fluorometers provides a non-intrusive method to determine the photosynthetic performance of autotrophic organisms. The DIVING-PAM was utilised to determine the photosynthetic efficiency of *in hospite* zooxanthellae associated with six subtropical corals, and to determine the effects of higher-than-normal seawater temperature in combination with summer irradiance on the photosynthetic apparatus of two common coral species in northern New South Wales, Australia. Mean maximum quantum yield of the six coral species (located *in situ*) ranged between 0.60-0.68, which was generally consistent with previously-reported efficiency rates from other location. Results from laboratory experiments in which *Turbinaria mesenterina* and *Pocillopora damicornis* were exposed to four different temperatures (21, 26, 28 and 30ºC) and two light intensities (100 and 400 µmol photon m^{-2} s^{-1}) showed a significant reduction in photosynthetic efficiency in *P. damicornis* exposed to temperatures ≥ 28ºC in high light intensities, and in *T. mesenterina* bathed in 30ºC in high light conditions. However, a similar response was found in replicates exposed to 21ºC and high light, which could indicate cool-water stress. *P. damicornis* appears to be more susceptible to bleaching than *T. mesenterina*. Fragments of *T. mesenterina* exposed to 30ºC and high light showed a significant rise in photoinhibitory quenching compared to fragments exposed to maximum seawater temperature (26ºC) at this location in the presence of summer irradiance. This may indicate that longer exposure to these bleaching conditions may result in host/symbiont disassociation in this species.

6.2 Introduction

The mutualistic association between scleractinian corals and single-celled photosynthetic microalgae known as zooxanthellae has been extensively studied (Sorokin 1982; Baker and Rowan 1997; Baker *et al.* 1997; Rowan 1998; Baker 2003; Knowlton and Rohwer 2003; Visram and Douglas 2006). This association has enabled the growth of extensive coral reefs (e.g. Great Barrier Reef [GBR], Australia) at locations where nutrients in the ocean are limiting (Stanley and Swart 1995). Through photosynthesis the zooxanthellae provide an essential energy resource to the coral and, in exchange, the host provides the symbiont with nutrients for photosynthesis as well as protection from the environment. Synthesised carbon compounds produced via photosynthesis are translocated to the cells of the host, which contribute to its nutritional budget (Muscatine *et al.* 1981). Muscatine (1990) estimated that up to 95% of translocated photosynthetic products such as amino acids, sugars, complex carbohydrates and small peptides are supplied to the host from the symbiont. It has been estimated that carbon products from the zooxanthellae adequately meets the hosts energy requirements for respiration, growth and the production of organic material such as coral mucus (Spencer Davies 1984).

Coral bleaching, which results in the disassociation between the coral host and the algal symbiont, has important ramifications for coral reef structure and function. With the loss of symbiosis due to prolonged stress such, as elevated temperatures, the host is more susceptible to disease (Cervino *et al.* 1998; Kushmaro *et al.* 1998; Richardson *et al.* 1998b; Toren *et al.* 1998; Banin *et al.* 2000; Thompson *et al.* 2001; Rosenberg and Ben-Haim 2002; Ben-Haim *et al.* 2003a; Thompson *et al.* 2005) and has reduced reproduction competency (Szmant and Gassman 1990; Ward *et al.* 2000). Therefore, recruitment is potentially compromised following mass-bleaching events. Additionally, if stress conditions continue long enough, coral mortality will occur; up to 65% mortality was reported following the 1998 mass bleaching episode at nearshore reefs within in the GBR (Berkelmans and Oliver 1999). Lesser (1997) indicated that the expulsion of zooxanthellae by the host was due in part to the production of toxic molecules (oxygen radicals) by the symbiont, which caused cellular damage in the coral host. It is therefore important to gain a greater understanding of the mechanisms that result in coral bleaching and the effects of temperature and light stress on the algal symbiont.

6.2.1 Measuring photosynthetic efficiency using fluorescence quenching analysis: Pulse Amplitude Modulating (PAM) Fluorometer

6.2.1.1 Quantum yield estimates

The measurement of Chlorophyll (Chl) fluorescence from Photosystem II (PSII) of autotrophic organisms using the Pulse Amplitude Modulating (PAM) fluorometer is an extremely sensitive and non-intrusive method for the determination of photosynthetic efficiency. Important information can be obtained regarding photosynthetic reactions when plants and algae are exposed to various environmental stress conditions (Schreiber 2004). Absorbed light is funnelled through the Chl antennae pigments into the reaction centres (RCs) of the PSI (Photosystem I) and PSII, where energy conversion takes place. This Chl is incorporated in the form of pigment-protein complexes in the thylakoid membrane and photosynthetic energy conversion involves charge separation at the PSI and PSII RCs. Excited energy that causes Chl to move from ground state to its singlet state ^{1}Chl can be relaxed via several pathway; these include, the re-emission of energy as fluorescence, de-excitation through thermal dissipation, and electron transfer through the RCs. Fluorescence emission is complementary to the other mechanisms; they are referred to as photochemical quenching (qP) and non-photochemical quenching (NPQ) of Chl fluorescence. The measurement of Chl fluorescence can provide important information regarding the kinetics of the photosynthetic process and these parameters have been experimentally proven to be a reliable measure of PSII quantum yield for a variety of photosynthetic organisms (Schreiber 2004; Klughammer and Schreiber 2008).

With the recent development of the Diving-PAM (Heinz Walz GmbH, Effeltrich Germany), Chl fluorescence analysis has been used to determine photosynthetic responses of marine organisms *in situ* when stressed by increased temperature and irradiance (Beer *et al.* 1998; Jones *et al.* 1999; Ralph *et al.* 1999; Okamoto *et al.* 2005). Additionally, other fluorescence equipment such as the Mini-PAM and the Imaging-PAM have been used to measure fluorescence emission from stressed coral holobiont in a laboratory setting (Warner *et al.* 1996; Jones *et al.* 1998; Warner *et al.* 1999; Jones *et al.* 2000; Hill *et al.* 2004; Ralph *et al.* 2005).

Pulse Amplitude Modulating fluorometers measure the quantum yield of the photochemical energy conversion using different modulated light intensities. Firstly, when a dark-adapted sample is illuminated by a weak far-red light-source, minimum Chl fluorescence (F_o) is determined, as all the reaction centres are oxidised and able to accept electron from the Chl antennae pigments. Secondly, a saturation light is applied to the sample for < 1 second, which fully reduces the electron transport chain between PSII and PSI, lowering photochemical quenching to zero and inducing maximal Chl fluorescence (F_m). Because changes in non-photochemical quenching are assumed to be too slow to become effective within the short period of the saturation pulse, maximum quantum yield of the sample can be determined using these fluorescence variables. The difference between F_o and F_m is called variable fluorescence (F_v) and the maximum quantum yield of a dark-adapted sample can be determined using the ratio of these fluorescence measurements:

$$\text{Maximum quantum yield (MQY)} = F_v/F_m = (F_m\text{-}F_o / F_m) \qquad \text{(Equation 1)}$$

Important information can be obtained when measuring fluorescence of light-adapted samples. However, because some of the reaction centres may be reduced, F_o is not used. Rather F is used which accounts for the fluorescence emission due to ambient light. Thus in equation 1, F_o is replaced with F. Additionally, F_m is substituted with light adapted maximum fluorescence yield (F_m') and the effective quantum yield of a light-adapted sample can be determined (see Ralph and Gademann 2005 for further explanation). Effective quantum yield of a light adapted sample is determined by the equation:

$$\text{Effective quantum yield } (\Phi_{PSII}) = (F_m' - F) / F_m' \qquad \text{(Equation 2)}$$

6.2.1.2 Rapid light curves and electron transport rate

Rapid light curve (RLC) is a pre-installed routine of the Diving-PAM, which enables the determination of the relative electron transport rate (rETR) of photosynthetic organisms at different light intensities. The use of rETR (Φ_{PSII} x PAR x 0.5, where: PAR is photosynthetically active radiation; and, 0.5 accounts for the distribution of irradiance between PSI and PSII), is appropriate because an accurate absorption coefficient for corals has not been determined for many coral species (Hoegh-Guldberg and Jones 1999; Ralph *et al.* 2002; Hoogenboom *et al.* 2006). Rapid light curves are plots of

rETRs versus actinic irradiance, which are calculated by subjecting samples to increasing light intensities prior to a saturation pulse. Information regarding the photosynthetic capacity of the PSII can be determined over a wide range of light intensities. As indicated by Ralph and Gademann (2005), RLCs are similar to the traditional photosynthesis-irradiance curves (P-E), which are used to measure changes in O_2 and CO_2 to describe acclimation of the photosynthetic apparatus to a range of light levels. However, Ralph and Gademann (2005) indicated that RLCs do not reach steady state conditions prior to each light-step measurement of fluorescence; therefore, the Φ_{PSII} and rETR determined by the PAM underestimates the optimal efficiency of the system. By analysing data and subsequent graphs (which require curve fitting, see Ralph and Gademann 2005) produced by the routine, important information regarding limitation to the photosynthetic apparatus such as minimum saturation irradiance (E_k) and maximum rate of relative electron transport ($rETR_{max}$) can be determined.

During a RLC routine, F is determined following an initial short, dark-adaptation period, and then the actinic light is increased in eight steps. The initial intensity is determined by the operator setting the light curve intensity (LC-INT) from 1 (low light) to 5 (moderate light) for a nominated period (generally 10 s in duration). Following the prescribed actinic light intensity period, F is measured. A 0.8 s saturation pulse is then applied which reduces the acceptor side of the reaction centre and maximum fluorescence is recorded prior to the next increase in actinic light intensity. Data recorded by this routine enable the estimation of rETR following each actinic increment using the equation:

$$rETR = \Phi_{PSII} \times PAR \times 0.5 \qquad \text{(Equation 3)}$$

As indicated by Ralph and Gademann (2005), in order to compare RLCs the data require curve fitting using the equation recommended by Platt (1980):

$$P = P_s (1 - e^{-(\alpha E_d / P_m)}) \qquad \text{(Equation 4)}$$

where: P_s is the scaling factor defined as the maximum potential rETR; P_m is the photosynthetic capacity at saturating light; α the initial slope of the RLC before the onset of saturation; and E_d the downwelling irradiance (400-700nm) (Ralph and Gademann 2005). Using these parameters, rETRmax and E_k can be estimated using the equations:

$$rETR_{max} = P_s(\alpha/[\alpha+\beta])(\beta/[\alpha+\beta])^{\alpha/\beta} \text{ and} \quad \text{(Equation 5)}$$

$$E_k = rETR_{max}/\alpha \quad \text{(Equation 6)}$$

where α and β are the rise in the cure in the light-limiting region and the slope of the RLC when PSII efficiency declines, respectively.

6.2.1.3 Non-photochemical quenching analysis

Non-photochemical quenching is complementary to Chl fluorescence emission and serves to dissipate excitation energy away from the light harvesting complex (LHC). Three components of NPQ have been identified according to their relaxation kinetics in darkness following a period of illumination. These include: energy-dependent quenching (qE); state-transition quenching (qT); and photoinhibitory quenching (qI). Energy-dependent quenching is the main component of NPQ and results from a build up of a transthylakoid pH gradient of the xanthophyll cycle (Demmig-Adam *et al.* 1996), which generally relaxes within seconds to minutes when samples are placed in the dark (Muller *et al.* 2001). When photosynthetic organisms are exposed to excessive light (experienced during the middle of the day), qE provides a feedback control mechanism that dissipates absorbed light energy away from the PSII RCs. The second component of NPQ, qT, relaxes within minutes to tens of minutes following darkness and is an important mechanism in algae, as it aids in maximising photosynthetic efficiency of both PSII and PSI. State transition results in the redistribution of absorbed energy away from PSII to PSI and *vice versa*, possibly through the rearrangement of chlorophyll protein complexes that result from phosphorylation of the LHC associated with PSII RCs (Haldrup *et al.* 2001). Photoinhibitory quenching is the final component of NPQ, which remains following the quenching of the other NPQ components. Relaxation of inhibition occurs very slowly from tens of minutes to hours. Inhibition energy is thought to damage the reaction centres of the PSII when the capacity of the protective mechanisms (qE and qT) is exceeded, resulting in the damage to D1 proteins associated with the PSII RCs (Krause and Weis 1991).

Previous determination of the components of NPQ have used chemical inhibitors such as 3-(3,4-dichlorophenyl)-1,1-dimethylurea (DCMU), which block electron transfer from Q_A^- to the plastoquinone pool, by binding to the Q_B site of the D1 protein and inhibiting the formation of the ΔpH across the thylakoid membrane (Krause and Weis

1991; Hill *et al.* 2005). However, as indicated by Hill *et al.* (2005), the addition of DCMU results in the destruction of corals. Alternatively, the different components of NPQ can be determined on the basis of differences in relaxation times in the dark (Krause and Weis 1991). This method has previously been used to determine the NPQ characteristics of photosynthetic symbionts associated with scleractinian corals (Gorbunov *et al.* 2001).

Using the Diving-PAM, the objective of is study was to gain an understanding of photosynthetic kinetics of zooxanthellae associated with subtropical scleractinian corals that inhabit reefs adjacent to the north coast of New South Wales (NSW). More specifically, this research aimed to: i) provide a baseline estimate of the quantum yield and electron-transport- rate of healthy, common, subtropical corals in the Solitary Islands Marine Park (SIMP), NSW, Australia; ii) determine the effect temperature and light have on the photosynthetic efficiency of *Turbinaria mesenterina* and *Pocillopora damicornis* corals; iii) determine ($rETR_{max}$) and E_k of *T. mesenterina* and *P. damicornis* at different temperatures when exposed to low light and high light, in order to determine if short term (days) photoacclimation occurred; and iv) determine the components of NPQ associated with *T. mesenterina* when exposed to different temperatures and light intensities combinations.

6.3 Methods

6.3.1 Field estimates (Quantum yield and RLCs)

Split Solitary Island (SSI, 30.23°S, 153.17°E, Fig. 3.1), was the site where all *in situ* fluorescence measurements were completed and from which the coral samples were collected. On the 4th November 2005, MQY estimates were recorded from six common subtropical eastern Australian coral species (*Acropora solitaryensis*, *Favia favis, Goniastrea Australensis*, *P. damicornis*, *T. mesenterina* and *T. radicalis*), at 10 m depth using SCUBA equipment and the Diving-PAM. The fibre-optic cable of the Diving-PAM was placed in the surface holder and, with the aid of the attached rubber bands, this holder was located onto four replicates colonies from each species for a period of 2 min (quasi-dark-adaption period) prior to the saturation pulse and subsequent fluorescence measurements (Fig. 6.1). These data only estimated maximum quantum

yield because each sample was only dark-adapted for 2 min (completing the recommended 20-min adaptation period (Ralph *et al.* 1999) would have required many repeated dives). However, previous experience indicated that a 2-min period produced similar results to those obtained for a 20-min period (data not shown). The tip of the fibre-optic cable, which was fastened inside the surface holder, was located 5 mm away the coral tissue during all measurements. Maximum quantum yield estimates were recorded following the saturation pulse and data were stored in the instrument's memory. Using a previously-calibrated quantum sensor attached to the Diving-PAM, maximum PAR intensity at 10 m was recorded.

Rapid light curves were completed for four replicate *T. mesenterina* colonies in order to determine the effective quantum yield and rETR at different light intensities *in situ*. Data were compared with results from samples exposed to laboratory conditions (see below). The surface holder was placed onto the coral colonies for 10 s prior to the initiation of the RLC routine. The staged actinic light intensities were determined prior to the *in situ* measurements using the LI-COR quantum sensor attached to the LI-250A light meter (Li-Cor, Lincoln USA) and the actinic settings on the Diving-PAM were adjusted accordingly. Data were averaged for all staged actinic intensities and, using Sigmaplot (2001) V7.0 and the curve fitting equation, $rETR_{max}$ and E_k were determined.

Figure 6.1: Example of the PAM fibre-optic cable mounted inside the surface holder and placed on a *Turbinaria mesenterina* colony. Photo Matthew Harrison

6.3.2 Laboratory experiment 1

6.3.2.1 Field collection and acclimation

Replicate *T. mesenterina* and *P. damicornis* fragments were collected from SSI to monitor photosynthetic response at different temperature and light intensity combinations. As limited space and lighting was available to complete the experiment in the controlled environment room at the National Marine Science Centre (NMSC) Coffs Harbour, two collection periods and subsequent experiments were carried out.

Samples of *T. mesenterina* and *P. damicornis* were collected in July and September 2005 respectively, at a depth of 10 m using a hammer and chisel to fragment each colony. Five colonies from each species were placed into separate plastic bags, *in situ*, which were filled with seawater and transported to the laboratory in two 60-L plastic containers filled with seawater. During the collection dives, the PAR at 10 m was recorded using the quantum sensor attached to the Diving-PAM. In July, light intensity ranged between 100-125 µmol photon m^{-2} s^{-1} during the late morning of a cloudless day and reached 280 µmol photon m^{-2} s^{-1} during September. Previously, measurements at this site during summer indicated that PAR intensity can be as high as 525 µmol photon m^{-2} s^{-1} at this depth (unpublished data).

On return to the laboratory, the coral colonies were further broken into approximately 10, 50-mm long portions and each fragment was placed into an individual large plastic container in an outside raceway. Each container was supplied with flow-though seawater and aerated. The raceway was shaded from direct sunlight using 70% shade cloth, which reduced the incident PAR intensity to a maximum of approximately 100 µmol photon m^{-2} s^{-1}. These samples were monitored for two weeks and only the portions of each colony that showed signs of tissue recovery at the fragmented margins, with no decrease in colour or any signs of tissue sloughing, were used.

6.3.2.2 Experimental design

The purpose of this experiment was to compare the photosynthetic response in zooxanthellae that were subjected to different temperature and light intensity combination, as well as to monitor them for any short-term photoacclimation response. The experiment included two light intensities, low light (LL) and high light (HL), (100 and 400 µmol photon m^{-2} s^{-1}, respectively) each in combination with four water

temperatures: 21°C and LL (experimental control, similar to *in situ* conditions during collection); 21°C and HL (light intensity control); 26°C and LL (temperature treatment); 26°C and HL (summer control); 28 and 30°C and HL (high temperature and light treatments). A total of six fragments from four colonies (24 individual fragments) were used during each experiment for each species. Fragments were randomly placed into individual, previously conditioned, 2.5 L food-safe plastic containers filled with 2 L of seawater and placed into the treatment water baths, which were maintained at 21°C during the setup stage of the experiment. The seawater within each container was aerated using a 20-mm air stone. The seawater in the containers was changed daily.

Two 250 Watt (W) and three 400 W, 10,000 Kelvin metal halide lights (no UV radiation) were used to supply the LL and HL treatments, respectively. During the experiments, the corals were exposed to a 10-h d^{-1} photoperiod. Jagar 100 W submersible water heaters were used to maintain water bath temperatures. These water heaters were previously calibrated to the required temperature using a TPS pH Cube thermometer. Throughout the experiments, the water baths were maintained within ± 0.4°C of the required temperatures.

6.3.2.3 Maximum quantum yield estimates

The night before the first fluorescence measurements, the water heaters were switched on allowing the seawater temperature within each container to rise to the required temperatures, (this took up to six hours in the 30°C treatments). On the morning of the Day 1 of each experiment, and following far-red illumination (Lastek Industries 740 nm filter), MQY measurements were taken for each control fragment using the Diving-PAM, which was connected to a laptop and controlled via the WINControl program (Heinz Walz GmbH, Effeltrich Germany). During these measurements, the fibre-optic cable was placed within the acrylic holder, which maintained a constant 5-mm gap between the end of the cable and the coral samples. Maximum quantum yield estimates were recorded for each fragment during the morning of Day 1, through to Day 4, for the *T. mesenterina* experiment, but only during Day 1 and Day 2 for the *P. damicornis* experiment. This difference in protocol was due to excessive loss in fragment colour, excessive mucus production, discoloration of the aquarium water, and subsequent mortality in the *P. damicornis* fragments in the 28 and 30°C HL treatments. Following the initial morning MQY measurements, the metal halide lights were switched on.

6.3.2.4 Rapid light curves

Rapid light curves (minimum one hour light adapted) were completed on all fragments at 1, 2, 4, 8, 24, 48, 72 and 96 hrs after the commencement of the *T. mesenterina* experiment, and 1, 2, 4, 8 and 24 hrs following the commencement of the *P. damicornis* experiment. As indicated above, many coral fragments in the *P. damicornis* experiment died between the Day 2-3 of the experiment, resulting in the loss of all 30°C HL replicates and some in the 26 and 28°C HL treatments. Before each RLC routine, each replicate was exposed to 10 s of darkness and subsequent fluorescence measurements recorded light affected fluorescence estimates (F and F_m'). Further, fluorescence values were recorded following each staged 10 s actinic light exposure and subsequent saturation pulse (SP). WINControl software calculated the Φ_{PSII}, rETR, NPQ and other parameters for each replicated routine. Following the completion of each experiment, data were imported into Sigmaplot V7 and the curve fitting procedure was completed to determine $rETR_{max}$ and E_k values.

6.3.3 Laboratory experiment 2

6.3.3.1 Field collection and acclimation

In order to further investigate the effects of temperature and light intensity on the PSII of the zooxanthellae associated with *T. mesenterina*, the components of NPQ were determined using the modified, dark-relaxation procedures used on plant leaves (see Melkonian *et al.* 2004; Kościelniak and Biesaga-Kościelniak 2006) and corals (Gorbunov *et al.* 2001). Four *T. mesenterina* colonies from reefs adjacent to SSI were fragmented *in situ* using a hammer and chisel in July 2007. These large fragments were placed into individual zip-lock bags filled with seawater and placed into 60-L plastic containers during transport to the laboratory, where they were further fragmented into 50-mm long portions and placed into large plastic containers in an outside raceway that was covered with 70% shade cloth. Flow-through seawater was supplied to each container and the water was aerated. Fragments were monitored for two weeks and only those that displayed coral tissue growth at the broken margins and no signs of stress (tissue loss and bleaching) were used in the NPQ analysis experiment.

6.3.3.2 Non-photochemical quenching analysis

Five fragments from each colony were used in this experiment, in which fragments were exposed to the same light and temperature combinations as in experiment 1. Individual fragments were removed from the outside plastic containers and placed into a water bath within the controlled environment room. Flow-through seawater maintained at 21°C was circulated for 12 hrs whilst the fragments were kept in darkness prior to NPQ quenching analysis. Individual fragments were then placed into a 2.5-L food safe container filled with 21°C seawater and placed into the water bath. The water temperature within the container was increased and reached the required treatment temperatures within approximately 1 hour.

Following temperature equalisation, each fragment was transferred into a modified 2.5-L food safe container (large portions of the sides removed) within a 35-l glass aquarium filled with 15 L of seawater (Fig. 6.2). The seawater was maintained at the required treatment temperatures using a Jagar 100 W water heater and a 30 W powerhead provided water circulation over the fragments. The lid of the container was modified by attaching conduit tubing, which enabled the end of the fibre-optic cable to be placed 5 mm above the coral fragments (Fig. 6.2). Each fragment was exposed to 10 s of far-red light (740 nm) prior to dark-adapted fluorescence measurements.

Following the dark-adapted measurements, each replicate was exposed to 6 min of actinic light (reaching steady state), from the diving-PAM 20 W halogen lamp at either actinic intensity (LC-INT) 4 and 7, depending on light treatment, which corresponded to 100 and 400 µmol photon m^{-2} s^{-1}, respectively. Light-adapted fluorescence measurements were then recorded followed by 10 and 60 min dark-relaxation fluorescence measurements. This procedure was replicated four times at each temperature and light intensity combination.

The components of NPQ were determined within each treatment by calculating the difference between the initial dark-adapted maximum fluorescence measurement (F_m), the light-adapted maximum fluorescence (F'_m) and subsequent F_m measurements following 10 (F_{m10}) and 60 (F_{m60}) minutes of darkness, relative to F'_m.

Total NPQ was determined using the equation:

$$NPQ = (F_m - F_m') / F_m' \text{ (Schreiber 2004)} \quad \text{(Equation 7)}$$

Additionally, individual components of NPQ (qE, qT and qI) were determined using the following equations,

$qE = (F_{m(10)} - F_m') / F_m'$ (Equation 8)

$qT = (F_{m(60)} - F_{m(10)}) / F_m'$ (Equation 9)

$qI = NPQ - (qE + qT)$ (Fig. 6.3) (Equation10)

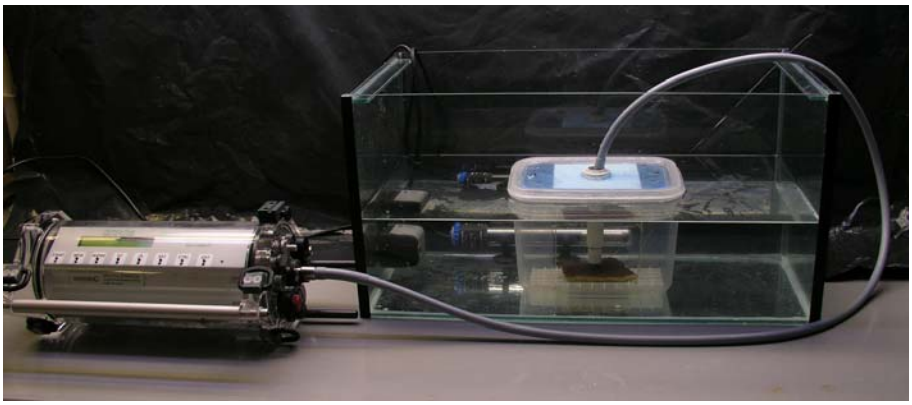

Figure 6.2: Diving PAM and fibre-optic housing used to measure relaxation kinetics of replicate *Turbinaria mesenterina* fragments exposed to different temperatures.

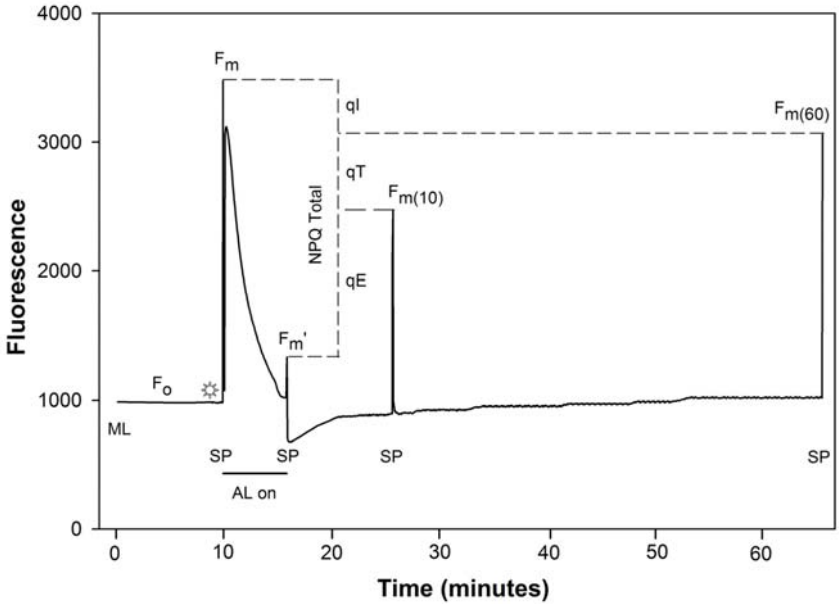

Figure 6.3: Example of Chl fluorescence induction kinetics. Components of NPQ (qE, qT and qI) are indicated: SP-saturation pulse; AL-actinic light; and sun symbol indicates far-red illumination (740nm).

6.3.4 Statistical analysis

6.3.4.1 Field estimates

Maximum quantum yield data were tested for normality and equality of variance using Anderson-Darling and Levene's tests, respectively. One-way ANOVA was used to test for difference in MQY between common subtropical coral species found within the SIMP. Additionally, a *post hoc* (Tukey HSD) test was used to determine if there were any differences in MQY between species. Rapid light curve routines recorded for *T. mesenterina* samples *in situ* were exported to Sigmaplot V.7 software and curve-fitting procedures completed, which determined $rETR_{max}$ and E_k for *T. mesenterina* colonies. These measurements were used as baseline data and subsequently compared against laboratory experiment data.

6.3.4.2 Laboratory experiment 1

6.3.4.2.1 Maximum quantum yield

During the experiment, it was noted that some of the fragments in the higher temperature baths either recorded quantum yield values of zero or coral tissue had sloughed-off prior to MQY measurements. In order to maintain a balanced design for subsequent analyses, average values from the remaining treatment replicates were used where data was missing (Underwood 1997). Additionally, as suggested by Underwood (1997) statistical analyses results from these balanced designs were compared with the results for analyses where the replicate number was reduced to the minimum number of replicates remaining (i.e. from n = 4 to n = 3 within each treatment). As there was no difference in the two sets of analyses, the balanced data set results are reported.

Prior to analysis, where necessary data were double square-root transformed to meet ANOVA assumptions. Two-way ANOVA tested the hypotheses that there was no difference in MQY between replicate fragments exposed to: i) high temperature (21ºC LL vs 26ºC LL); ii) high light (26ºC LL vs 26ºC HL); and iii) temperatures of 1 and 2°C above average, maximum SIMP seawater temperature (26ºC HL vs 28ºC HL and 26ºC HL vs 30ºC HL, bleaching treatments), over a short period of time (days). Pairwise (Tukey HSD) tests were performed in order to detect where significant differences occurred between treatments over time. Results from the analysis were adjusted to account for the inclusion of average values where replicates were lost. The error degrees

of freedom, adjusted sums-of-squares and F-ratio were modified according to the total number of replicates remaining within the treatments and the probability levels were determined using F-distribution tables (Underwood 1997).

6.3.4.2.2 Rapid light curve

To investigate short-term photoacclimation potential of *T. mesenterina* and *P. damicornis* to elevated temperature in the presence of summer irradiance, second-order polynomial regressions were fitted to $rETR_{max}$ and E_k time-series plots. If short-term photoacclimation (days) occurred during these experiments, E_k values should approach ambient irradiance (100 and 400 umol m^{-2} s^{-1} for the LL and HL treatments, respectively). Therefore, optimal performance of the PSII would be shown by a higher $rETR_{max}$ at ambient light intensities.

6.3.4.3 Laboratory experiment 2

6.3.4.3.1 Non-photochemical quenching analysis

One-way ANOVA tests were conducted on the data for total NPQ and the components of NPQ (qE, qT and qI) to determine if light, temperature and the combination of the two factors caused a significant response in the PSII of *in hospite* zooxanthellae. Statistical analysis was done to determine if there was: i) a temperature effect (21ºC LL vs 26ºC LL); ii) a light intensity effect (26ºC LL vs 26ºC HL); and iii) a combined light intensity and temperature affect (26ºC HL vs 28ºC HL and 26ºC HL vs 30ºC HL, bleaching treatments). Bleaching conditions in this study are defined as being > 1 ºC above mean summer maximum (26.66 ºC within the SIMP) in the presence of high (summer) irradiance 400 umol m^{-2} s^{-1}.

6.4 Results

6.4.1 Field measurements

In situ MQY ranged between 0.60-0.68 for all coral species evaluated, with *Acropora solitaryensis* recording the highest value (Fig. 6.4). One-way ANOVA indicated that MQY was significantly different ($F_{5, 18} = 4.49$, $p = 0.008$) between species. However, Turkey pair-wise comparison indicated that this difference was due to the higher MQY value of *A. solitaryensis* compared to *T. mesenterina* and *T. radicalis* at the $p < 0.05$

significance level. MQY values for all other species were not significantly different from each other (Fig. 6.4).

Mean rETR values increased following each increase in actinic irradiance but there was no plateau and subsequent down-regulation during this procedure, which can affect the calculations of $rETR_{max}$ and E_k (Ralph and Gademann 2005). $rETR_{max}$ determined by curve-fitting the RLC graph was 73.89 μmol electrons m^{-1} s^{-1}, and minimum saturating irradiance was 456.7 μmol photons m^{-1} s^{-1}. The curve-fitting procedure showed a significant concordance ($r^2 > 0.99$, $p < 0.0001$) with the mean rETR values generated by the RLC.

6.4.2 Laboratory experiment 1

6.4.2.1 Maximum quantum yield

Mean MQY values recorded during the experiments showed some similarities for each coral species within both the controls and treatments combinations. Following one day of exposure to experimental conditions the 21°C HL fragments showed a decline in photosynthetic efficiency, particularly for *T. mesenterina*, relative to the experimental control (21°C LL). This pattern of decline was similar to that for the sample exposed to high temperature and high light (Fig. 6.5). This decline in MQY in the 21°C HL treatment for both species may be due to low temperature bleaching (P. Ralph personal communication). As the aims of this experiment were to determine the effects of higher-than-normal temperature and irradiance on the photosynthetic efficiency of the PSII, the data for 21°C HL treatment were removed from subsequent analysis as this treatment potentially confounded the results.

Tissue loss and subsequent mortality was observed in five *T. mesenterina* fragments during the experiment. Within the HL treatments, tissue sloughed off one replicate at 28°C and all the replicates 30°C between the second and third day. During the *P. damicornis* experiment, seven fragments died within 36 hrs including four replicates at 30°C HL, two at 28°C HL and one at 26°C HL, resulting in the premature termination of this experiment. At the beginning of the experiment mean MQY within the experimental controls (21°C LL) was 0.68 ± 0.003 (SE) and 0.69 ± 0.007 for *T.*

mesenterina and *P. damicornis*, respectively. There was a decline in MQY after 24 hrs within the *T. mesenterina* experimental controls and this lower yield was maintained during all subsequent measurements (Fig. 6.5). Yield values recorded from the *T. mesenterina* fragments exposed to summer temperature (26°C) and low light was not significantly different to the experimental control data (Table 6.1; Test i), but there was a significant time effect; MQY declined significantly between 72 and 96 hours in the controls and 26°C LL treatments (Table 6.1; Test i). In contrast, MQY was significantly higher in the *P. damicornis* control compared to the replicates held at 26°C and this trend was consistent though time (Table 6.1; Test i). Results for both species confirmed a significant light effect (26°C LL vs. 26°C HL; Test ii) and a significant decline in MQY within the 30°C HL treatment compared to the summer HL control within *T. mesenterina* experiment and between both 28°C and 30°C treatments compared to 26°C HL control during the *P. damicornis* experiment (Table 5.1; Test iii).

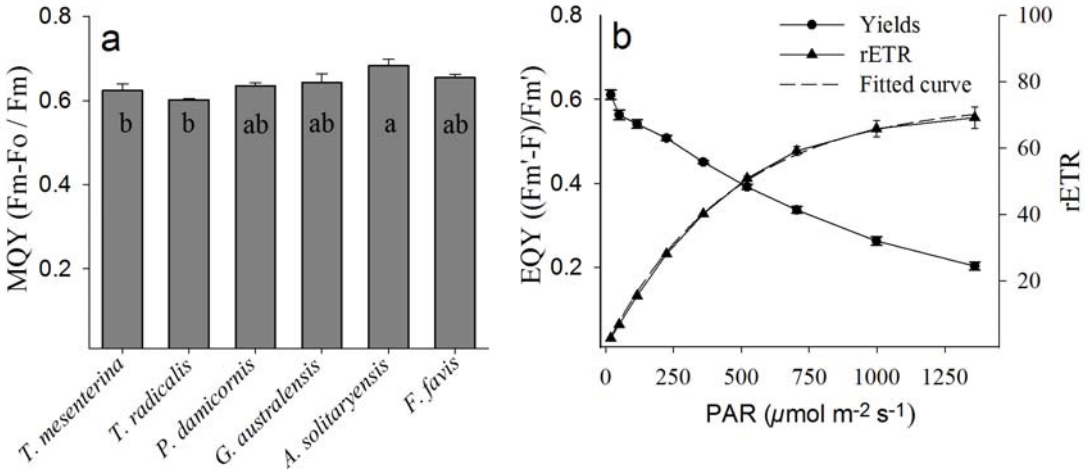

Figure 6.4: a) Maximum quantum yield (±SE) for six common coral species found within the SIMP. Tukey's pair-wise comparisons: significant differences indicated by different letters at the $p < 0.05$ confidence level. b) Calculated rETR (±SE) and effective quantum yield (±SE) as a function of actinic irradiance from RLC recorded from four *T. mesenterina* colonies.

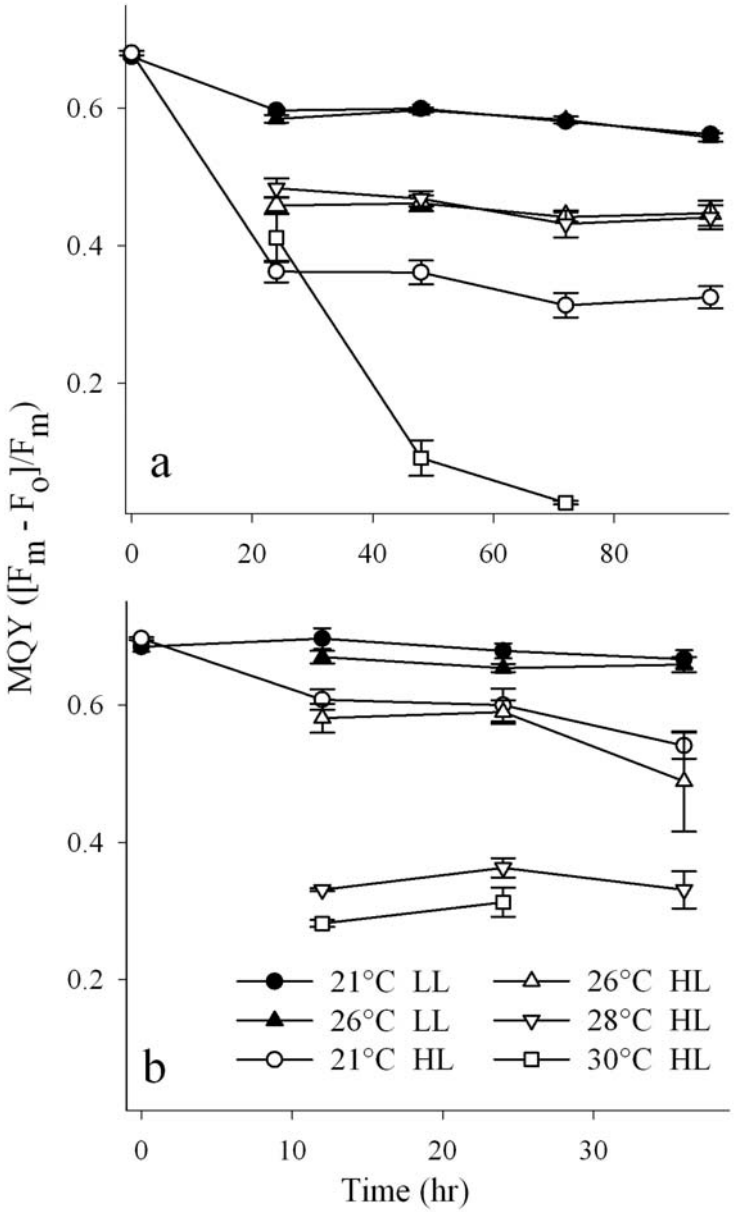

Figure 6.5: Maximum quantum yield (MQY) values (± SE) recorded over time from two subtropical coral species a) *Turbinaria mesenterina*, and b) *Pocillopora damicornis* exposed to different light (100 and 400 μmol photon m^{-2} s^{-1}; LL and HL, respectively) and temperature (21, 26, 28 and 30°C) combinations.

Table 6.1: Two-way ANOVAs, which tested for differences in maximum quantum yield (MQY) between: i) 21°C LL & 26°C LL (temperature effect); ii) 26°C LL & 26°C HL (irradiance effect); and iii) 26°C HL & 28°C HL, 26°C HL & 30°C HL (temperature effect at high irradiance). Significant Tukeys pair-wise comparison indicated, with highest MQY shown from left to right. (») $p < 0.001$(›) $p < 0.05$

Species	Test		F (df)	*p*	Tukey's tests
T. mesenterina	i)	Temp	1.46 (1,31)	0.238	
		Time	24.61 (3,31)	0.000	24 = 48 = 72 » 96 hr,
		Temp x Time	0.85 (3,31)	0.482	
	ii)	Light	352.36 (1,31)	0.000	LL » HL
		Time	2.74 (3, 31)	0.065	
		Light x Time	0.92 (3,31)	0.446	
	iii)	Temp	257.24 (2, 35)	0.000	26 = 28 » 30°C,
		Time	59.80 (2, 35)	0.000	
		Temp x time	40.61 (4, 35)	0.000	
P. damicornis	i)	Temp	4.53 (1. 23)	0.047	
		Time	1.89 (2 23)	0.179	
		Temp x Time	0.44 (2, 23)	0.6	
	ii)	Light	32.08 (1, 23)	0.000	LL » HL
		Time	0.76 (2, 23)	0.482	
		Temp x Time	1.29 (2, 23)	0.301	
	iii)	Temp	197.53 (2, 23)	0.000	26 » 28 › 30°C
		Time	3.56 (1, 23)	0.075	
		Temp x Time	0.36 (2, 23)	0.704	

6.4.2.2 Rapid light curves

Sub-saturation irradiance (E_k) and $rETR_{max}$ calculated from the RLC curve-fitting procedures tended to be highest initially (within the first few hours of light exposure), declining throughout the first 24 hours in both the controls and treatments for both coral species (Fig. 6.6). For *T. mesenterina*, there was a decline in both parameters in the summer control (26°C LL, Fig. 6.6 a). Within the 26 and 28°C HL treatments, an initial decline was observed during the first 24 hrs followed by a gradual increase after 48 hrs (Fig. 6.6 b, c).

In contrast, within the *P. damicornis* 26°C LL treatment (Fig 6.6 e), E_k and $rETR_{max}$ declined initially then increased over the 24 hour sampling period; there was a general trend for E_k to decline through time in the high light and high temperature combinations

(Fig. 6.6 f-g). Sub-saturation irradiance did not fall below 400 μmol m^{-2} s^{-1} in any of the control or treatment fragments of *P. damicornis* during the experiment (Fig. 6.6 e-h).

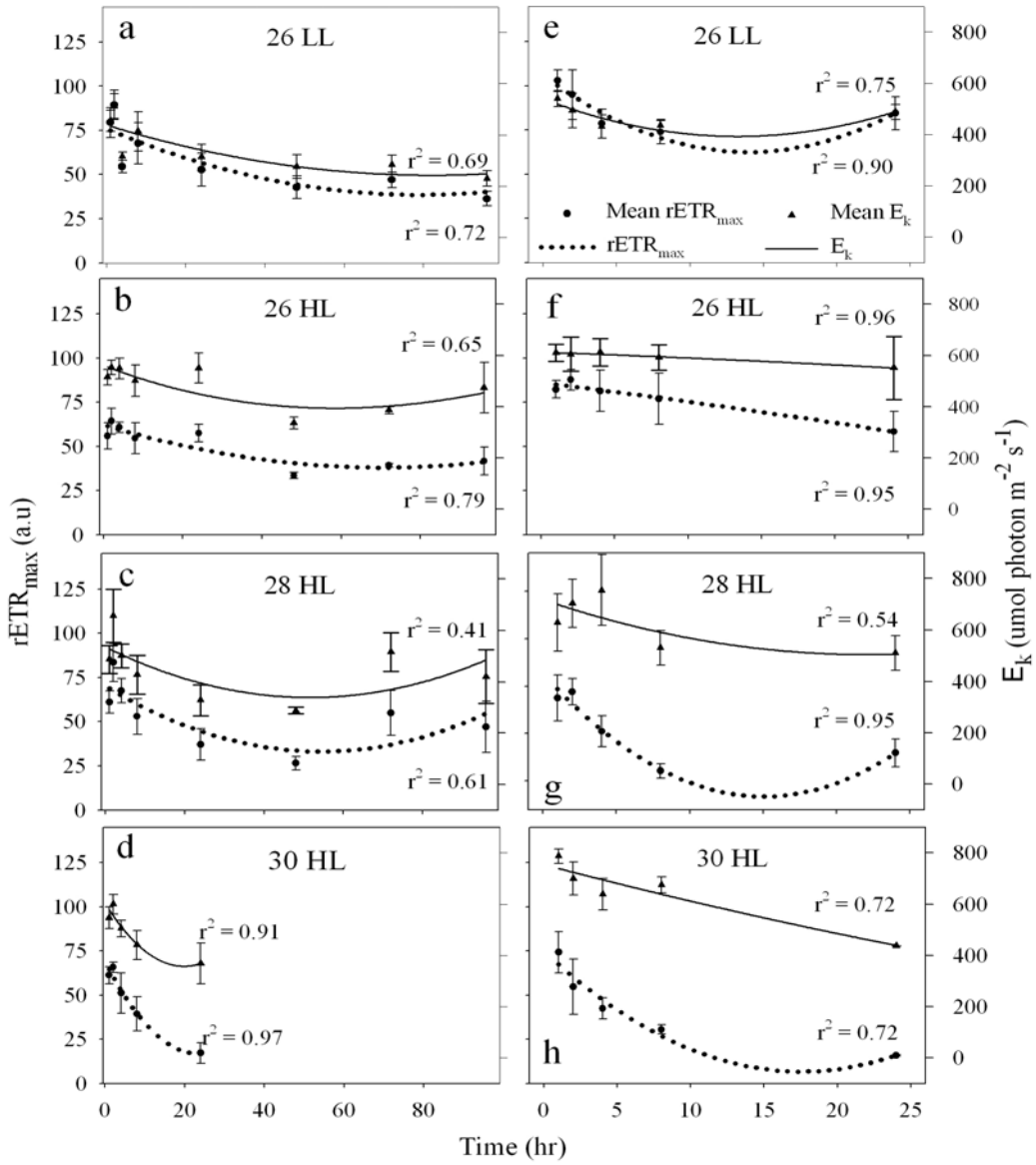

Figure 6.6: Change in E_k and $rETR_{max}$ over time from *Turbinaria mesenterina* (a-d) and *Pocillopora damicornis* (e-h) fragments exposed to different light and temperature combinations: 26°C LL (a,e); 26°C HL (b,f); 28°C HL (c,g), and 30°C HL (d, h). LL and HL represent 100 and 400 μmol m^{-2} s^{-1}, respectively. *T. mesenterina* and *P. damicornis* experiments were conducted over 96 and 24 hours, respectively. E_k and $rETR_{max}$ polynomial curve-fitted lines shown by solid and dotted lines, respectively.

Regression analysis for each variable (E_k and $rETR_{max}$) within each light and temperature combination showed a generally good fit to the data (i.e. high r^2 values Fig. 6.6). However, within the *T. mesenterina* 28°C HL treatment (Fig.6.6 c) the model only accounted for 41% of the variation in E_k. All regression models were significant at the $p < 0.05$. There was a curvi- linear or negative-linear relationship between each variable though time; however, E_k did not reach steady state in any light/temperature combination. Steady-state irradiance is indicated when E_k approaches and maintains ambient irradiance through time with high PSII efficiency (i.e. higher rETRmax).

Split-plot analysis, which compared the rate-of-change in $rETR_{max}$ within each treatment through time, demonstrated that there was no significant increase in PSII efficiency rate in any of the light/temperature combinations, with a significant decline in $rETR_{max}$ within 30°C HL treatment for both *T. mesenterina* ($F_{1, 6} = 33.73$, $p = 0.001$) and *P. damicornis* ($F_{1, 6} = 25.10$, $p = 0.002$). However, within the *T. mesenterina* 28°C HL treatment (Fig.6.6 c), following a decline in photosynthetic efficiency, some adaptive capacity was observed.

6.4.3 Laboratory experiment 2

6.4.3.1 Non-photochemical quenching

Mean NPQ was of similar magnitude between replicates exposed to control conditions (21°C LL) and high seawater temperature at low light (26°C LL). As expected, there was a significant increase in total NPQ at the higher PAR intensity (26°C LL vs 26°C HL, $F_{1, 7} = 194.85$, $p = 0.000$). Total NPQ was not significantly different between the summer control (26°C HL) and the bleaching treatments (28°C HL & 30°C HL), but the components of NPQ (qE, qT and qI) varied (Fig. 6.7). There was a non-significant increase in qE quenching between 26°C HL and 28°C HL, with 30°C HL treatment qE of similar magnitude to the summer control (Fig. 6.7). State-transition quenching differed between the summer control (26°C HL) and the two bleaching treatments but this was not significant. One-way ANOVA which tested for a bleaching effect between the summer control (26°C HL) and treatments maintained at higher than average summer temperatures showed a significant difference in photoinhibitory quenching (qI; $F_{2,11} = 6.83$, $p = 0.016$), with this difference associated with significantly higher values in the 30 °C HL treatment (0.797 ± 0.05 [± SE]) compared to the 26°C HL control (0.577 ± 0.05). There was no

significant difference between 28°C & 26°C and between 28°C & 30°C maintained at high light irradiance.

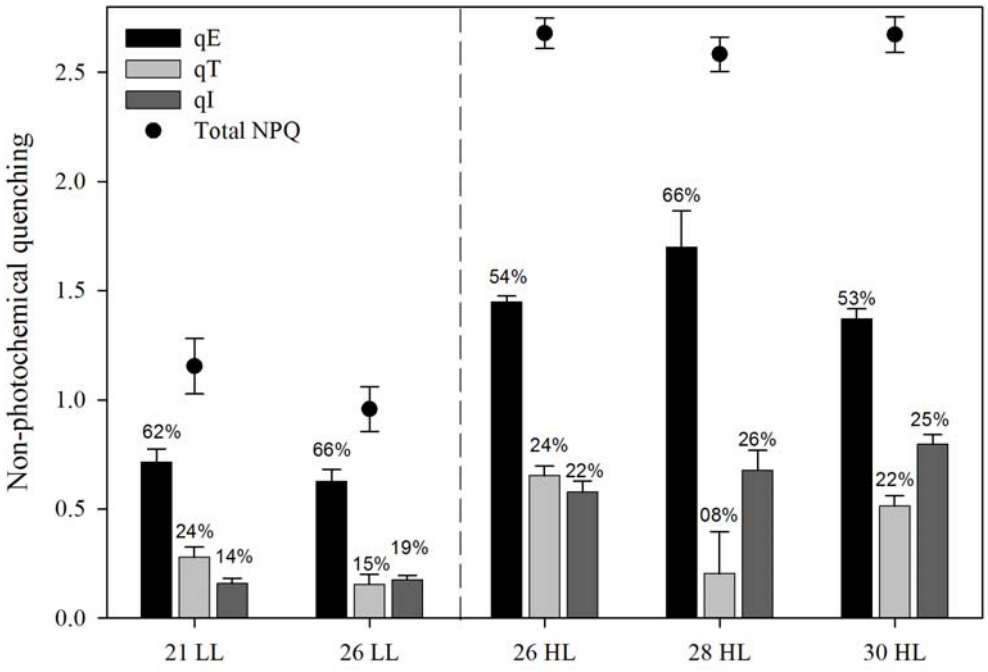

Figure 6.7: Comparison of NPQ analysis determined under different light/temperature combinations. 21°C LL (experimental control), 26°C LL (temperature control), 26°C HL (summer control) and two bleaching treatments, i) 28°C HL (1°C above average maximum summer temperature [AMST]) and ii) 30°C HL (3°C above AMST). Components of NPQ; (qE) energy-dependent quenching, (qT) state-transition quenching and (qI) photoinhibitory quenching. LL and HL represent PAR values of 100 and 400 µmol m^{-2} s^{-1} respectively. Error bars are standard error of the mean. Average percentage contribution of total NPQ from all components indicated above bars.

6.5 Discussion

The results from this study show that summer light intensity in the presence of high temperatures (28°C and 30°C) had a significant effect on the photosynthetic efficiency of the *in hospite* zooxanthellae associated with *Turbinaria mesenterina* and *Pocillopora damicornis*. However, cooler temperatures (21°C) and high light also produced similar results. Temperatures greater than 26°C, in the presence of summer irradiance had a greater effect on *P. damicornis* than *T. mesenterina*, suggesting that *P. damicornis* may be more susceptible to chronic photoinhibition, which may lead to bleaching.

6.5.1 Field measurements

Maximum quantum yields recorded during this study were of similar magnitude to measurements previously reported by Okamoto *et al.* (2005) who report values between 0.61 to 0.70 for 68 coral species. However, comparing MQY for congenics between this study and that by Okamoto *et al.* (2005), indicates some differences. Maximum quantum yields for *Turbinaria* species measured during this study ranged between 0.60 ± 0.003 (± SE) for *T. radicalis* and 0.62 ± 0.005 for *T. mesenterina*, whereas MQY for *Turbinaria* corals recorded at Sekisei Lagoon, Okinawa, Japan averaged 0.66 ± 0.001. Yields for *Goniastrea* sp. were also lower in this study (0.64 ± 0.002) compared to the Okinawa study (0.67 ± 0.003). This dissimilarity may be due to a number of reasons; including where the fibre-optic cable was placed on the sample during fluorescence measurements. During this study, the fibre-optic cable was located on the upper sun-lit surface of the corals, whereas measurements were collected from shaded areas on corals at Sekiseo Lagoon. A difference in photosynthetic efficiency have been observed previously between regions directly exposed to light compared to shaded areas (Ralph *et al.* 1999). Lower efficiency rates in full sun exposed samples are associated with down-regulation of MQY of the PSII, which quickly dissipates during lower light condition, which may have contributed to the difference in MQY measured during this study compared to Okamoto *et al.* (2005) findings.

6.5.2 The effect of light and temperature on PSII efficiency

Maximum quantum yields give an indication of the activity and efficiency of PSII, where a decline is indicative of down-regulation or photoinhibition. During each MQY estimate subsequent to Day 1, there was a significant decline in photosynthetic efficiency in the

corals exposed to the high light treatments. As indicated by Gorbunov *et al.* (2001), chronic photoinhibition established following periods of supraoptimal irradiance only recovers following several hours of low irradiance. Early morning MQY estimates showed a slight progressive decline in PSII efficiency, which may indicate that repair to damaged protein was not occurring. A more natural diel light regime may have enabled repair of degraded reaction centres of the PSII following maximum irradiance. Additional studies considering this limitation would enable further understanding of the effects of high temperatures in combination with summer irradiance levels.

Some PSII RCs may have become chronically photoinhibited and may have remained permanently dysfunctional during subsequent days of high irradiance exposure. This may explain why, following the Day 1 measurements, MQYs recorded from *T. mesenterina* in high light treatments declined then tended to remain consistent within the 26 and 28°C temperature treatments. Chronic inhibition was also noted for the replicates held at 30°C. For *P. damicornis*, a significant reduction in MQY was recorded following 10 hrs of high light exposure, with increased non-photochemical quenching occurring in both the 28 and 30°C treatments compared to the summer control (26°C - HL). This may indicate that *P. damicornis* is more susceptible than *T. mesenterina* to temperatures greater than summer averages. These results are consistent with previous studies which have shown differences in bleaching susceptibility among taxa. Marshall and Baird (2000) found that pocilloporids, including *P. damicornis*, were highly susceptible to bleaching, whereas *Turbinaria* spp. were relatively resistant to bleaching during the 1998 GBR mass-bleaching event.

Complete tissue loss was observed in all *P. damicornis* replicates in the high light treatments (28 and 30°C) within the first 36 hrs. At the same time period, no tissue loss was observed in any of the *T. mesenterina* replicates; although all 30°C replicates died between Day 2 and Day 3. These results indicate that summer light intensity in combination with 30°C water temperature induced a bleaching response in *T. mesenterina*, whereas a significant reduction of PSII efficiency was found in *P. damicornis* at both 28 and 30°C in combination with high light. This further suggests that the thermal threshold for *P. damicornis* is lower than that for *T. mesenterina* at this location.

During both experiments, replicates held at 21°C and high light showed a decline in photosynthetic response, which was similar to fragments exposed to higher-than-average summer temperatures combined with high light. Saxby *et al*. (2003) showed that cool water (≤ 20°C) and high irradiance resulted in an increased photoihibitory response in *Montipora digitata*; this response was similar to that of corals exposed to warmer-than-normal temperatures and summer irradiance. Decrease in photosynthetic performance may indicate increased sensitivity to photoinhibition, which might lead to bleaching and/or increased zooxanthellae respiration in response to low temperature and high irradiance (Steen and Muscatine 1987). With temperature fluctuating between 20-26°C (see Chapter 5) during summer months, when irradiance is at its maximum, a decline in coral pigmentation could conceivably result from either high or low temperatures within the SIMP, assuming field responses are equivalent to the responses documented in the laboratory studies.

6.5.3 Photoacclimation – Rapid Light Curves

Recent research has shown that, following several weeks of exposure to low light, corals tend to acclimate to ambient conditions through the synthesis or biochemical conversion of pigments or cells that alter the structure of the light harvesting complex (LHC). This optimises the performance of the photosystem relative to ambient irradiance. However, during this study E_k was initially higher than 400 μmol m^{-2} s^{-1} in all treatments, even within the low light controls. This result is inconsistent with the study by Anthony and Hoegh-Guldberg (2003). They found that *T. mesenterina* fragments acclimated to low pre-experimental irradiance (30 μmol m^{-2} s^{-1}), and when exposed to higher irradiance, initial E_k increased asymptotically from below 100 μmol m^{-2} s^{-1} and reached steady-state levels within 8-10 days. In contrast, during this study, initially E_k was higher than the pre-treatment irradiance (100 μmol photon m^{-2} s^{-1}) in all light/temperature combinations and then declined in all *T. mesenterina* and *P. damicornis* treatments. Difference in the results between the two studies might be attributed to the length of time the respective samples were exposed to pre-treatment irradiance. During this study, coral samples were only acclimated to setup irradiance for two weeks. In contrast, a four week pre-acclimation period was adopted in the previous study (Anthony and Hoegh-Guldberg 2003).

The magnitude of E_k may have also been overestimated due to the low α estimates determined from the RLC curve-fitting procedure. Ralph and Gademann (2005) indicated

that, by increasing the number of actinic irradiance steps that are closer to the ambient light levels (i.e. pre-treatment irradiance (100 µmol photon m^{-2} s^{-1}), a more precise estimate of α and subsequently Ek determination is achieved. During this study only one stepped-intensity level was lower than pre-treatment irradiance and as a consequence insufficient data in the light-limited region of the curves resulted in an underestimation of α values. Changing the light curve intensity (LC-INT) setting on the DIVING-PAM from level 3 to level 2 would have enabled additional data from the light-limiting region of the curve. However, there would have been insufficient irradiance to ensure saturation of the reaction centres. Down regulation of PSII was only achieved at light intensities higher the 1300 µmol photon m^{-2} s^{-1} and this magnitude was only achieved with LC-INT set to 3. By increasing the actinic factor setting (AL-FACT) from 1 to 1.20 whilst selecting LC-INT level 2 would have enabled additional data at low irradiance with an increased intensity range over the eight incremented irradiance steps (i.e., from 20 to 2000 µmol photon m^{-2} s^{-1}). This protocol may provide adequate information at pre-saturation irradiance levels whilst ensuring saturation of the reaction centres at higher light levels. However, this protocol requires further testing to validate the procedure.

Alternatively, results from this study may indicate that *T. mesenterina* and *P. damicornis* are light limited during periods of low light (i.e. during winter) with limited acclimation of the LHC. Coral polyps are normally extended during the day and active feeding, by the host, may meet nutritional requirements during periods low light conditions.

6.5.4 Non-photochemical quenching

Non-photochemical quenching is complementary to Chl fluorescence and provides mechanisms to dissipate excessive absorbed light energy away from the LHC of PSII. This study showed that, with increased irradiance, there was approximately a 2.5-fold increase in NPQ, with all components of NPQ (qE, qT and qI), generally increasing at a similar magnitude. Energy-dependent quenching remained an important mechanism for excessive energy dissipation for all treatments and contributed to between 53 - 66% of the total NPQ, with state transition quenching accounting for between 8 - 23% (Fig 6.8). Following 60 min of relaxation the remaining component of NPQ indicates the level of photoinhibition that occurred after 6 min of control and treatment irradiance. Photoinhibitory quenching ranged between 13-26% of the total NPQ for all light/temperature combinations, which corresponds to the amount of dynamic inhibition associated with damage to the DI proteins

in PSII, and/or chronic photoinhibition (degradation of D1 proteins) associated with high light exposure (Gorbunov *et al.* 2001). However, Gorbunov *et al.* (2001) indicated that chronic photoinhibition occurs when coral samples are exposed to irradiance levels ≥ 1500 μmol photon m^{-2} s^{-1} on shallow reef environments. In hard corals associated with subtropical reefs in eastern Australia, chronic inhibition irradiance might be much lower than this level, as the ambient light environment is considerably lower than corals associated with shallow tropical reefs. Maximum PAR measured during a clear summer day at 10 m at SSI was 525 (unpublished data) compared to PAR intensities greater the 2000 μmol photon m^{-2} s^{-1} for shallow tropical reefs (Brown *et al.* 1999).

Corals exposed to 30ºC and HL, showed a significant increase in qI, suggesting that, if these fragments were exposed to longer periods of treatment conditions, further oxidative damage to the photosynthetic apparatus may result. This is supported by the study by Hill *et al.* (2005) study that showed NPQ significantly increasing through time in *P. damicornis* exposed to a combination with high temperature and high temperature (32 ºC and 475 μmol photon m^{-2} s^{-1}). Further research is required to understand the effect higher than normal temperature in combination with summer irradiance, over extended periods, on SIMP corals.

This study has provided an indication of the photosynthetic performance of common coral species associated with subtropical reefs adjacent to eastern Australia. Overall, MQY values recorded for six species were similar to those recorded at other location; however, some differences were shown within genus. The effects of higher-than-normal seawater temperature in combination with summer irradiance had a significant effect on the photosynthetic efficiency of the two common coral species studied. *Pocillopora damicornis* appears to be more susceptible to bleaching compared to *T. mesenterina*, which is consistent with findings of previous studies. Evaluation of the components of NPQ from *T. mesenterina* samples exposed to different light/temperature combinations showed a significant inhibitory effect at 30°C in the presence of high light. However, the effect of long-term exposure to these conditions on the photosynthetic performance warrants further investigation.

CHAPTER 7 SPATIAL AND TEMPORAL PATTERNS OF EASTERN AUSTRALIA SUBTROPICAL BENTHIC COMMUNITIES: MONITORING CHANGE IN SCLERACTINIAN CORAL COVER

7.1 Abstract

Scleractinian corals associated with mainland subtropical benthic communities in eastern Australia form a veneer over the rocky substratum. However, on the western side of Lord Howe Island (LHI), coral accretion has occurred forming a fringing reef. During this study, data on benthic community composition were gathered using videotape transects from seven locations extending from southern Queensland (Flinders Reef 27°S, 153.5°E) to northern New South Wales (Black Rock, South West Rocks 31°S, 153.1°E) and at LHI (31.5°S, 159.1°E), a World Heritage listed island located 600 km east of mainland Australia. The aims of the research were to determine benthic community composition, explore latitudinal differences in benthic and coral assemblages and determine if there has been a decline in coral cover over small (years) and large (decades) temporal scales. This study revealed strong latitudinal differences in benthic ($F_{17,103}$ = 12.16, P = 0.001) and coral assemblages ($F_{4,103}$ = 3.136, P = 0.039) and, interestingly, community composition at some sites was more similar to those hundreds of kilometres away than to that of neighbouring reefs. *Acropora* species dominated the reefs adjacent to Flinders Reef and North Solitary Island (Solitary Islands Marine Park) and throughout the LHI lagoon, with a greater cover of dendrophyllids with increasing latitude and proximity to mainland Australia. Within the SIMP, a significant shift in benthic composition occurred at some sites through time; however, the coral community remained consistent over a 3-year period. Decadal comparisons also indicated that hard coral cover was generally stable at a regional scale, but small-scale differences were apparent within locations.

7.2 Introduction

Scleractinian (hard) coral communities extend from 11°S (northern Great Barrier Reef [GBR]) to as far south as 31.5°S (northern New South Wales [NSW]) along the eastern seaboard of Australia. On northern NSW reefs, corals generally do not form true coral reefs; rather colonies are observed attached to hard rocky substratum (Veron *et al.* 1974; Harriott and Banks 2002). However, high-latitude coral reefs have formed along the Lord Howe Rise, which is located 600 km east of mainland Australia, with reef accretion found at Elizabeth and Middleton reefs and on the western side of Lord Howe Island (LHI). Coral communities found south of the GBR are composed of a suite of tropical, subtropical and temperate species. As indicated by Harriott and Banks (2002), coral species richness declines with increasing latitude along the east coast of Australia. Flinders Reef (27°S), which lies 5.5 km to the north of Moreton Island, southern Queensland, comprises 119 hard coral species (Harrison *et al.* 1998), which represents a 50% decline in species richness relative to the southern GBR. Additionally, there is also an abrupt decrease in species richness south of the Solitary Islands Marine Park (SIMP; Harriott and Banks 2002). Whilst fewer coral species are associated with high-latitude reefs along the east coast of Australia, coral cover is comparable to that of the GBR, with up to 45% cover observed at Flinders Reef, island-associated reefs within the SIMP and within the LHI lagoon (Harriott *et al.* 1994; Harriott *et al.* 1995; Harrison *et al.* 1998).

Previous studies on eastern Australia subtropical reefs were conducted over small spatial scales and, when combined show latitudinal differences in benthic community composition. Harriott and Banks (2002) hypothesized that the lack of true coral reef formation along the east coast of mainland NSW and the abrupt decline in coral species richness were due to the combination of physical (temperature, light availability, currents, storm events, etc.) and biological (larval dispersal, competition for space, reduced growth rates and limited recruitment) factors, all interacting in a complex manner. Recently, additional stressors have been observed affecting hard coral within this region including: increased predation by crown-of-thorn starfish (Harriott 1995); coral bleaching (Kitchener 1998; Edgar *et al.* 2003); and coral disease (Dalton and Smith 2006). In light of the recent increase in frequency of natural (see Harriott and

Banks 2002) and/or anthropogenic (Smith *et al.* 2008) disturbances along southeastern Australia, it is timely to revisit the status of subtropical benthic communities.

This research was completed in conjunction with coral stress assessment surveys, with the objective of gaining an understanding of the effect disturbances such as coral disease, coral bleaching and predation have on the subtropical coral community. More specifically, the aims of this research were to: (i) determine the benthic community structure on representative coral-dominated high-latitude island reefs in eastern Australia; (ii) explore latitudinal differences in the benthic and coral communities at these locations; (iii) determine if there is a trend for different coral species to dominate at different locations; (iv) determine if there has been a decline in coral cover between 2004 and 2006 at representative SIMP island reefs as a result of the exposure to coral stressors such as disease, bleaching and predation; and (v) determine if there has been a change in benthic community structure over decadal temporal scales.

7.3 Methods

7.3.1 Study Sites

Benthic community composition data from subtropical locations were collected between 2004 and 2006 from five locations along the east coast of Australia (Fig. 7.1): Flinders Reef (FR); Cook Island (CI); Solitary Islands Marine Park (SIMP); South West Rocks (SWR); and Lord Howe Island (LHI). Site selection and locations for SIMP, SWR and LHI have been described previously (see Chapter 4) and sites at Flinders Reef were located on the north-western and north-eastern side of a small emergent sandstone outcrop that is approximately 500 m long and 250 m wide. Two sites were investigated at Cook Island, one on the northern side and the other on the southern side of the island. All sites were of similar depth (8-14 m) with the exception of the four LHI lagoon sites, which were only 2-5 m deep.

7.3.2 Benthic community structure

Previous research on eastern Australian subtropical reefs used underwater videotape transects to determine the status of benthic community structure at locations dominated by scleractinian coral (Harriott *et al.* 1995). Video sampling provides a fast, simple, reliable and cost-effective method to sample sessile organisms (Carlton and Done 1995)

and was therefore also utilised during this study. Five 30-m transects were randomly positioned at each site and, using a Sony TRV 950 video camera in a waterproof housing, a SCUBA diver swam along each transect at a constant speed (0.1 m s^{-1}), approximately 50 cm above the substratum, with the camera pointed downwards. The total time required to complete each transect was approximately 5-6 minutes. Videotape recordings were downloaded onto an Apple Mac G5 computer and digital videos produced for each site. Digital clips from each site were burnt onto DVDs and archived in an air-conditioned store room.

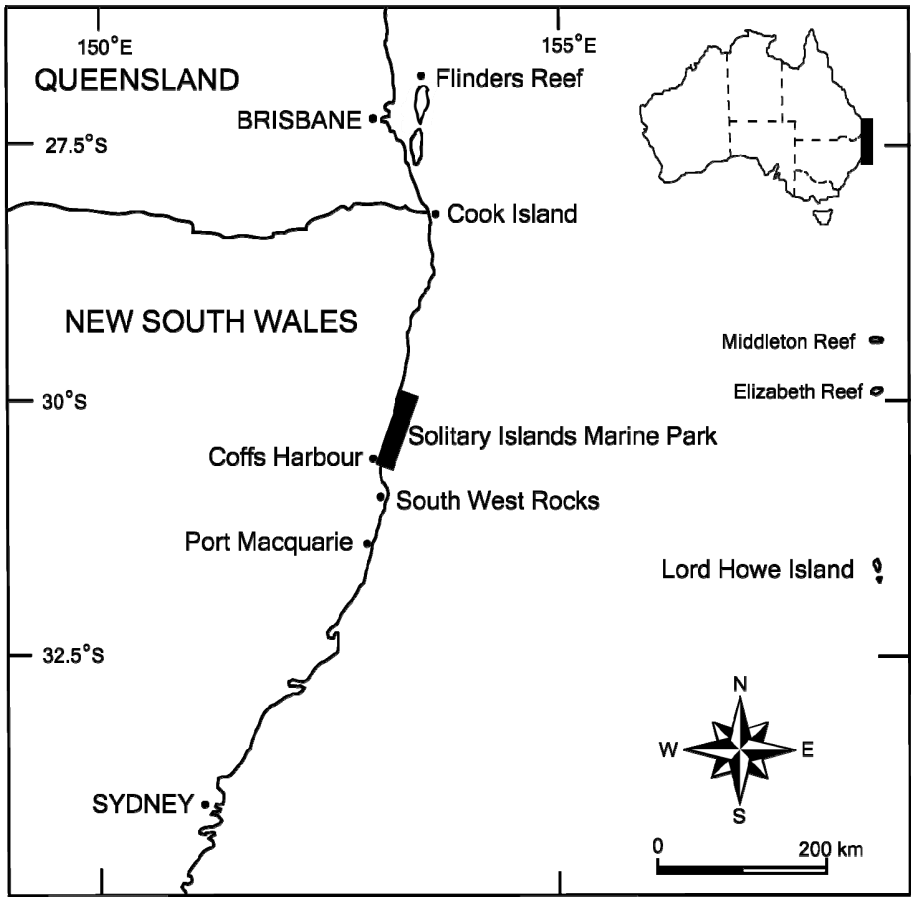

Figure 7.1: Map of eastern Australia showing the locations where subtropical benthic community composition was determined using replicate videotape transects. Sites within each location marked using Global Positioning System (GPS).

Initially, two transects from each site were viewed at normal speed and a comprehensive list of benthic categories was determined (Table 7.1). These categories complemented classifications previously used at these locations (Harriott *et al.* 1994, 1995, 1999; Harrison *et al.* 1998; Carroll 1999; Smith and Edgar 1999), thus enabling direct comparisons. Prior to analysis, different point methods, one point per frame (see Harriott *et al.* 1994, 1995) and five points per frame (Page *et al.* 2001), were compared to determine the most precise and cost-effective method of determining benthic cover. Two-way ANOVA indicated that there was no significant difference between the two methods in determining the coral community composition associated with subtropical reefs. Therefore, as the five points per frame method was significantly more time and cost effective, it was subsequently used in the study (data not shown).

Digital videos from each site were re-played on an Apple Mac G5 computer and recordings viewed on a liquid crystal display. Each transect was paused at predetermined intervals and benthic codes underlying five fixed points located within the transect area were recorded for 60 frames per transect. This resulted in a total of 300 points for each transect. The Coral Point Count with Excel extensions (CPCe) image software program (Kohler and Gill 2006), which provides a tool for the determination of benthic cover using transect photographs, was used in conjunction with the five points method. This program enabled raw data to be transferred to a Microsoft Excel spreadsheet where descriptive statistics were calculated automatically for each site. In order to maintain accuracy and eliminate observer biases, all videos were analysed by one analyst.

7.3.3 Statistical analysis

7.3.3.1 Latitudinal variation in benthic and coral community composition

All multivariate and univariate comparisons were performed using PRIMER 6.0 with PERMANOVA+ software. Initially, data from all sites were square-root transformed, which downweighted the contribution of common categories in relation to rarer categories, and similarities were calculated using the Bray-Curtis coefficient. The resulting resemblance matrix was analysed using a two-factor (location and sites nested within location) Permutational Analysis of Variance (PERMANOVA, Anderson *et al.* 2008). The null hypotheses tested were that there was no significant difference in benthic community structure over small spatial scales (hundred of metres to kms) and

large spatial scales (> 100 km) along the east coast of Southern Queensland and northern NSW. Non-Parametric Multidimensional Scaling ordination (nMDS) was performed to graphically represent the level of similarities/dissimilarities in community composition within and between sites, and hierarchical agglomerative cluster analysis was also performed to portray similarities between sites. Clusters were superimposed onto the nMDS to show samples that had a 65% similarity. This procedure resulted in nine similarity groups (hereafter denoted by S-Group 1 to S-Group 9). Similarities of percentages (SIMPER) analyses were used to determine which categories contributed approximately 50% of the dissimilarities between S-Groups and the categories that explained 50% of within S-Group similarities.

Abundance data for each coral family from each site were fourth-root transformed and normalised and a three-dimensional principal component analysis (PCA) was used to graphically display data. Eigenvectors of the variables (coral family vectors) were overlayed onto the resultant PCA biplot. Additionally, bubble graphs were superimposed onto the PCA family biplots, which displayed the percent cover of each coral family at all sites.

Univariate analyses were performed on coral cover and coral species richness data using the Euclidean distance matrix as the dissimilarity measure. Prior to analysis, single variables were tested for homogeneity of variance and heteroscadastic data were square-root transformed. The flexibility and robustness of the permutation-based analysis alleviates the necessity to normalise the data (Somerfield *et al.* 2008). Both *a priori* and *post-hoc* comparisons tested for overall and site differences, with significance values determined from 9999 and 999 unrestricted permutations of the square-root transformed data, respectively.

7.3.3.2 Temporal changes in SIMP benthic and coral community composition

Mean percent cover for all benthic and coral categories recorded during 2004 and 2006 survey periods were compared using multivariate and univariate analyses. Prior to analyses, data from each replicate transect were square-root transformed. Similarities in benthic and coral communities were determined via the Bray-Curtis similarity measure (Clarke 1993, Clarke and Warwick 2001). Using nMDS, a two dimensional plot of site centroids was generated, which graphically displayed differences in community structure between sites and years. Hierarchical agglomerative cluster analysis was also

Table 7.1: Benthic categories used during benthic community structure analysis.

Code	Description	Code	Description	Code	Description
Hard corals		**ECHIN**	*Echinophyllia aspera*	**COD**	*Codium* spp.
APAL	*Acropora palifera*	**MYCE**	*Mycedium elephantotus*	**UL**	*Ulvaceae* spp.
	Isopora cuneata	**ACANL**	*Acanthastrea lordhowensis*	**HALI**	*Halimeda* spp.
ASOL	*A. solitaryensis*	**ACANE**	*A. echinata*	**GAOT**	Green algae other
	A. glauca	**ACANB**	*A. bowerbanki*	**ECK**	*Ecklonia radiata*
	A. hyacinthus	**ACANH**	*A. hillae*	**SARG**	*Sargassum* spp.
ANAS	*A. nasuta*	**BLAST**	*Blastomussa merleti*	**DICT**	*Dictyotaceae* spp.
AVAL	*A. valida*	**SYPH**	*Syphyllia radians*	**BAOT**	Brown algae other
ACAL	*A. clathrata*	**HYDN**	*Hydnophora* spp.	**TURF**	Turfing algae
ACER	*A. cerealis*	**PLES**	*Plesiastrea versipora*	**Seagrass**	
ACYT	*A. cytherea*	**CYPHS**	*Cyphastrea serailia*	**SG**	Seagrass
AABR	*A. abrotanoides*	**CYPHC**	*C. chalcidicum*	**Other invertebrates**	
	A. robusta	**GONIA**	*Goniastrea australensis*	**ASCS**	Ascidian solitary
AFOR	*A. formosa*	**GONIF**	*G. favulus*	**ASCC**	Ascidian colonial
AYON	*A. yongei*	**GONIP**	*G. pectinata*	**Z**	Zoanthid
ALOV	*A. lovelli*	**PLAD**	*Plalygyra daedalea*	**ANL**	Large anemone
AFLO	*A. florida*	**PLAL**	*P. lamellina*	**ANS**	Small anemone
ABRA	A. branching	**LEPT**	*Leptastrea transversa*	**SPSM**	Sponge submassive
ACORR	A. corymbose/caespitose	**MONC**	*Montastrea curta*	**SPEN**	Sponge encrusting
APL	A. plate	**MONM**	*M. magnistellata*	**ECHC**	Crinoid
ADIG	A. digitate	**MONSP**	*Montastrea* spp.	**ECHE**	Echinoid
MONT	*Montipora* spp.	**LEPTO**	*Leptoria* spp.	**ECHA**	Asteroid
POC	*Pocillopora damicornis*	**FAVFL**	*Favites flexuosa*	**HYD**	Hydroid
POCV	*P. verrucosa*	**FAVAB**	*Favites abdita*	**BARN**	Barnacle
STYL	*Stylophora pistillata*	**FAVSP**	*Favites* spp.	**BRY**	Bryozoan
SERI	*Seriatopora hystrix*	**FAVIF**	*Favia favia*	**TWOR**	Tube worm
TRBF	*Turbinaria frondens*	**FAVIS**	*Favia* spp.	**GORG**	Gorgonian
	T. mesenterina	**Corallimopharia**		**OI**	Other invertebrate
TRBR	*T. radicalis*	**CORM**	Corallimorph spp.	**Substratum**	
TRBPA	*T. patula*	**Soft corals**		**BROCK**	Bare rock
TRBPE	*T. peltata*	**XEN**	*Xenia* spp.	**R**	Rock
TRBH	*T. heronensis*	**SCMS**	Soft coral massive	**S**	Sand
POR	*Porites* spp.	**SCEN**	Soft coral encrusting	**SED**	Sediment
GON	*Goniopora* spp.	**Macro algae**		**Dead coral**	
PSAS	*Psammocora superficialis*	**AMPA**	*Amphiroa anceps*	**RDC**	Recently dead coral
PSAH	*P.haimeana*	**ACOR**	Encrusting coralline algae	**DCA**	Dead coral algae
COSM	*Coscinaraea mcneilli*	**CORB**	*Corallina berteri*	**ODC**	Old dead coral
COSC	*C. columna*	**RAOT**	Red algae other	**Unknown**	
PAV	*Pavona* spp.	**CAL**	*Caulerpa* spp.	**UKN**	Unknown
LEPT	*Leptoseris hawaiiensis*	**TGRS**	*Chlorodesmis* spp.		

performed to portray similarities between centriods. Clusters were superimposed onto the nMDS to show centroids that had a 70 and 80% similarity. Benthic categories identified as contributing the first 50% of the difference in community structure within sites between years, were identified using the SIMPER procedure. Additionally, benthic community structure and coral community composition were evaluated using three-factor PERMANOVA, with pairwise contrasts completed where appropriate. The hypothesis tested was that there was no significant difference within these variables between sites within years and within sites between years. The significance level of all pairwise tests was adjusted for multiple comparisons using Bonferroni corrections.

7.4 Results

7.4.1 Latitudinal variation in benthic community composition

Scleractinian corals were observed at all locations; however, no hard corals were found at two sites adjacent to SWR (Bait Reef and Green Island). Results from the two-way PERMANOVA indicated that there was a highly significant difference in benthic assemblages between locations ($F_{4, 103} = 4.39$, $P = 0.001$) and between sites within locations ($F_{17, 103} = 12.16$, $P = 0.001$). Cluster and nMDS analysis showed that benthic communities formed nine distinct S-Groups at the 65% similarity level (Fig. 7.2). The nMDS and cluster overlay showed that two LHI lagoon sites (Erscott's Hole and Stephen's Hole) grouped towards the top left of the ordination (S-Group 1), with the two other lagoon sites clustering to the lower left (S-Group 2, Fig.7.2). The exposed LHI sites (Malabar Reef and Noddy Island) were more similar to the Cook Island sites (S-Group 6) than the LHI lagoon sites and grouped together between Flinders Reef sites (S-group 5) and the algal-dominated SWR sites (S-Groups 8 and 9). S-Group 7 consisted of SIMP midshelf island sites and the most southern mainland site Black Rock (SWR). Interestingly, the two sites from NSI within the SIMP (Anemone Bay- S-Group 3 and Trail Mooring - S-Group 4) were different to each other and all other sites (Fig. 7.2).

Benthic community composition associated with the groups that orientated towards the left and bottom of the ordination (S-Groups 1, 2 and 7) was dominated by hard corals (Fig. 7.2, Table 7.2), with substratum also a main component of these groups. S-Group 3, which appears geometrically located between S-Groups 2 and 7, coral cover was half that of the adjacent groups and large anemones occupied over 25% benthic cover (Fig. 7.2, Table 7.2).

The three-dimensional ordination generated by the PRIMER software (Appendix 5) indicates that S-Group 3 orientated closer to S-Group 4 than displayed in the above plot. Pairwise contrasts confirmed that the assemblage at Anemone Bay were more similar to the other NSI site (Trail Mooring, S-Group 4) than S-Groups 2 and 7 (data not shown). Coral cover in S-Groups 8 and 9 was minimal, containing only 2.0 and 0.0% cover, respectively. Algal cover within these groups was high, at 63.4 and 71.7%, respectively. Benthic communities in S-Group 5 and, to a lesser extent S-Group 6 showed an even distribution of the main benthic categories (Table 7.2).

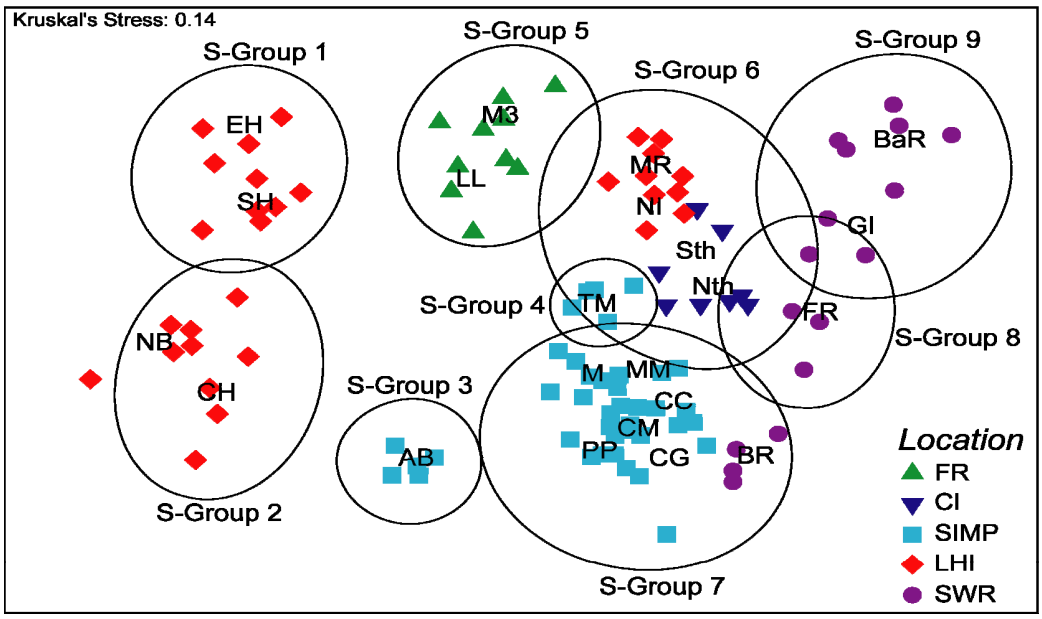

Figure 7.2: Non-parametric multidimensional ordination (nMDS) of benthic community composition in subtropical eastern Australian. Sites grouped according to 65% similarities (circles). Site abbreviations are orientated at the centroid and are: Flinders Reef – (LL) Laurieland, (M3) Mooring No 3; Cook Island – (Nth) Northern Mooring, (Sth) Southern Mooring; SIMP – (AB) Anemone Bay, (TM) Trail Mooring, (MM) Manta Mooring, (M) Midway Mooring, (CM) Crazy Maze, (CG) Coral Gardens, (PP) Pomfrey Point, (CC) Coral Corner; LHI – (NB) North Bay Wreck, (CH) Comet's Hole, (SH) Stephen's Hole, (EH) Erscott's Hole, (MR) Malabar Reef, (NI) Noddy Island; and SWR – (BR) Black Rock, (GI) Green Island, (BaR) Bait Reef, (FR) Fish Rock.

Table 7.2: Summary of mean percent benthic cover averaged within 65% similarity group (S-G) as defined by the cluster and nMDS analysis.

Benthic categories	S-G 1	S-G 2	S-G 3	S-G 4	S-G 5	S-G 6	S-G 7	S-G 8	S-G 9
Acroporidae	22.9	15.8	1.9	12.3	20.5	3.6	2.9	0.0	0.0
Agariciidae	0.0	0.0	0.0	0.0	0.0	0.1	0.0	0.0	0.0
Dendrophylliidae	0.0	0.0	0.1	0.4	2.0	2.7	25.0	0.9	0.0
Faviidae	0.4	0.4	0.4	4.0	3.5	5.6	8.0	0.3	0.0
Merulinidae	0.0	0.0	0.1	0.1	0.6	0.5	0.0	0.0	0.0
Mussidae	0.0	0.1	0.1	0.2	0.1	0.2	0.6	0.0	0.0
Pectinidae	0.0	0.0	0.0	0.0	0.0	0.1	0.0	0.0	0.0
Pocilloporidae	9.7	14.9	8.2	0.9	1.9	1.1	2.0	0.8	0.0
Poritidae	4.0	18.9	2.9	0.7	1.3	1.1	1.1	0.0	0.0
Siderastreidae	0.0	0.0	0.1	0.0	0.6	0.0	0.2	0.0	0.0
Hard coral total	**37.1**	**50.0**	**13.7**	**18.6**	**30.5**	**15.0**	**39.9**	**2.0**	**0.0**
Soft coral massive/encrust	20.5	0.5	0.4	0.7	12.6	6.6	2.4	0.3	1.1
Xenia spp.	3.8	2.3	0.4	0.1	6.4	0.1	0.2	0.0	0.0
Soft coral	**24.3**	**2.9**	**0.7**	**0.7**	**19.1**	**6.7**	**2.4**	**0.3**	**1.1**
Corallimorph spp.	**0.0**	**0.0**	**0.0**	**0.0**	**4.1**	**0.0**	**0.0**	**0.0**	**0.0**
Amphiroa anceps	0.0	0.0	0.1	2.3	2.3	0.4	0.1	0.0	0.5
Corallina berteri	0.0	0.0	0.1	1.3	1.8	0.2	0.1	0.2	1.9
Encrusting coralline algae	1.0	1.2	23.3	22.1	5.8	5.4	12.4	15.1	2.0
Red algae other	4.8	5.8	5.2	8.8	11.5	12.8	1.5	0.6	2.5
Red algae total	**5.8**	**7.0**	**28.7**	**34.5**	**21.4**	**18.7**	**14.1**	**15.8**	**6.8**
Caulerpa spp.	2.6	0.0	0.0	0.1	1.7	0.2	0.1	0.3	8.5
Chlorodesmis spp.	0.2	0.0	0.9	0.4	0.1	0.2	0.1	0.0	0.0
Codium spp.	0.0	0.0	0.0	0.3	0.5	0.2	0.0	0.0	0.0
Green algae other	1.5	0.6	5.0	7.6	1.5	0.7	0.6	4.5	0.0
Halimeda spp.	0.0	0.1	0.1	0.0	0.0	0.1	0.0	0.0	0.0
Ulvaceae spp.	0.0	0.0	0.0	0.0	0.0	0.0	0.0	0.0	0.0
Green algae total	**4.3**	**0.7**	**6.0**	**8.5**	**3.8**	**1.4**	**1.0**	**4.8**	**8.6**
Brown algae other	0.6	0.5	0.1	0.5	0.3	1.9	0.2	2.7	15.0
Dictyotaceae spp.	1.5	0.2	0.0	2.5	0.1	2.4	0.1	0.0	0.0
Ecklonia radiata	0.0	0.0	0.0	0.0	0.0	0.0	0.0	0.0	0.0
Sargassum spp.	0.0	0.0	0.0	0.0	0.0	0.0	0.0	0.0	5.7
Brown Algae total	**2.0**	**0.6**	**0.1**	**3.1**	**0.3**	**4.3**	**0.4**	**2.7**	**20.7**
Seagrass	1.1	0.5	0.0	0.0	0.0	0.0	0.0	0.0	0.0
Turf algae	0.0	0.0	3.2	15.5	6.9	37.3	13.0	40.1	35.6
Algal assemblage	**12.2**	**8.3**	**38.0**	**61.5**	**36.5**	**61.7**	**28.4**	**63.4**	**71.7**
Ascidian colonial/solitary	0.0	0.0	0.0	0.1	0.0	0.9	3.2	3.9	1.4
Asteriod	0.0	0.0	0.	0.1	0.0	0.1	0.0	0.0	0.0
Barnacle	0.0	0.0	0.1	0.1	0.1	0.8	1.1	3.1	0.0
Bryozoan	0.0	0.0	0.0	0.0	0.0	0.1	0.0	0.0	0.0
Crinoid	0.0	0.0	0.0	0.0	0.5	0.2	0.0	0.4	0.1
Echiniod	0.1	0.2	4.9	2.1	0.0	0.9	1.2	4.5	0.0
Gorgonian	0.0	0.0	0.0	0.0	0.0	0.0	0.0	0.0	0.0
Hydroid	0.0	0.0	0.0	0.0	0.0	1.0	0.0	0.0	0.0
Anemone large/small	0.9	3.7	28.4	1.4	0.1	0.4	0.1	0.0	0.3
Other invertebrate	0.0	0.0	0.4	0.0	0.1	0.0	0.1	1.8	0.4
Sponge	0.2	0.3	0.8	0.5	4.4	3.5	3.0	7.6	14.0
Tube worm	0.0	0.0	0.1	0.0	0.0	0.0	0.3	0.0	5.2
Zoanthid	0.0	0.0	0.1	0.4	1.3	0.0	0.6	0.0	0.0
Invertebrates total	**1.2**	**4.2**	**34.8**	**4.7**	**6.5**	**7.8**	**9.7**	**21.3**	**21.3**
Dead coral with algae	17.5	22.5	6.5	4.3	2.3	1.8	6.8	0.2	0.0
Old dead coral	0.0	0.0	0.5	0.0	0.0	0.0	0.1	0.0	0.0
Recently dead coral	0.2	5.2	1.7	1.5	0.5	0.2	1.0	0.0	0.0
Bare rock	0.0	0.0	1.5	3.0	0.0	0.4	3.6	2.8	0.4
Rubble	1.4	1.8	2.4	5.4	1.6	1.3	1.5	9.8	0.7
Sand - sediment	4.9	4.5	0.0	0.2	3.8	5.1	6.5	0.3	4.8
Substratum total	**24.1**	**34.0**	**12.5**	**14.4**	**7.3**	**8.8**	**19.5**	**13.1**	**5.9**

Table 7.3: Results from SIMPER analysis which shows the benthic categories which contributed to 50% of the similarities within each group. Percentage contribution for each category shown in parenthesis.

S-Group 1	**S-Group 2**	**S-Group 3**
Soft coral submassive (18.5%)	Dead coral with algae (21.1%)	Large anemone (17.3%)
Dead coral with algae (16.4%)	*Porites* spp. (14.9%)	Coralline algae (15.4%)
P.damicornis (9.2%)	*P. damicornis* (13.8%)	Dead coral with algae (7.6%)
A. palifera/I. cuneata (8.2%)		*P. damicornis* (7.2%)
S-Group 4	**S-Group 5**	**S-Group 6**
Coralline algae (13.2%)	Red algae other (11%)	Turf algae (24.2%)
Turf algae (10.6%)	*A. palifera/I. cuneata* (8.7%)	Red algae other (12.6%)
Red algae other (8.0%)	Xenia (8.0%)	Coralline algae (7.2%)
Green algae (7.1%)	Soft coral massive (7.9%)	Soft coral massive (5.9%)
Rubble (6.4%)	Turf algae (7.9%)	Sand (5.6%)
S-Group 7	**S-Group 8**	**S-Group 9**
Turbinaria fron/mes (14.4%)	Turf algae (24.8%)	Turf algae (24.4%)
Coralline algae (11.5%)	Coralline algae (13.8%)	Encrusting sponge (13.7%)
Turf algae (11.4%)	Rubble (10.85)	Brown algae other (13.0%)
Dead coral with algae (8.2%)	Encrusting sponge (10.0%)	

The SIMPER analysis, which compared the similarities within each group and dissimilarities between groups are represented in Table 7.3 and 7.4, respectively. Sites within S-Group 1 had similar soft coral, *Pocillopora damicornis* and *Acropora palifera/Isopora cuneata* cover, while S-Group 2 assemblages showed a consistent cover of dead coral with algae, *Porites* spp. and *P. damicornis*. Large anemones, coralline algae and *P. damicornis* consistently contributed to benthic community structure throughout Anemone Bay (S-Group 3), whilst at Flinders Reef (S-Group 5), red algae, *A. palifera/I. cuneata* and other cnidarians occupied the two sites. In contrast, *Turbinaria* spp. were well represented within S-Group 7 sites, with turf algae and other algae categories sharing similar coverage in S-Groups 6, 7 and 9 (Table 7.3).

Submassive soft coral and *Acropora lovelli* consistently had higher cover in S-Group 1 compared to all other groups (Table 7.4), whereas dead coral with algae and *Porites* spp. had higher cover in S-Group 2 relative to all other groups. Large anemones explained a high proportion of the dissimilarity between S-Group 3 and all other groups, whereas the difference between S-Group 7 and the other groups was primarily explained by the high cover of *Turbinaria* spp. and *Goniastrea australensis*. Submassive soft coral, encrusting sponge and a suite of algal categories, explained much of the dissimilarities between S-Groups 5, 6, 8 and 9, and between these S-Groups and the other S-Groups (Table 7.4).

Table 7.4: SIMPER analysis which indicates the benthic categories which contributed to the first 50% of the dissimilarities between the S-Groups determined using cluster and nMDS analysis. Acronyms defined in Table 7.1. Categories are listed in order of their percentage contribution to the dissimilarities between S-Groups. Categories listed to the left of each cell had a higher abundance within the S-Group listed down the left column, while categories listed to the right of the cells had a higher abundance within the S-Group listed at the top of the cell.

	S-Group 1	**S-Group 2**	**S-Group 3**	**S-Group 4**	**S-Group 5**	**S-Group 6**	**S-Group 7**	**S-Group 8**
S-G 2	SCSM POR RDC ALOV ASOL S AYON CAL							
S-G 3	ANL ACOR SCSM APAL ECHE ALOV TURF S	ACOR ANL POR DCA ECHE TURF AYON APAL						
S-G 4	SCSM ACOR TURF AABR APAL DCA POC ALOV	TURF ACOR POR DCA POC AABR GAOT BROCK	ANL AABR TURF POC DICT MONM AVAL BROCK					
S-G 5	DCA TURF ALOV SPEN ASOL APAL SCSM POC	POR DCA SCSM TURF POC APAL SPEN RDC	ANL APAL SCSM ACOR ECHE XEN CORM SPEN	APAL SCSM AABR ACOR XEN BROCK CORM GAOT				
S-G 6	TURF DCA SCSM POC ASOL ALOV XEN RAOT	TURF POR DCA POC RDC SCSM RAOT AYON	ANL TURF ACOR S SCMS POC GAOT ECHE	ACOR AABR GAOT TURF SCSM R S BROCK	TURF APAL XEN SCSM CORM S TRBF BAOT			
S-G 7	TBRF SCSM TURF ACOR APAL GONIA ALOV POC	TBRF TURF POR ACOR POC GONIA DCA TBRR	ANL TBRF S GONIA TURF TRBR GAOT POC	TRBF AABR GAOT RAOT S TRBR GONIA DICT	TRBF APAL SCSM RAOT XEN GONIA BROCK CORM	TRBF TURF RAOT GONIA SCSM ACOR BROCK DCA		
S-G 8	TURF SCSM DCA ACOR ASOL SPEN POC APAL	TURF DCA POR ACOR POC SPEN RDC R	ANL TURF DCA POC SPEN ASCS GAOT POR	ABRA TURF RAOT GAOT SPEN DCA ASCS DICT	TURF APAL RAOT SCSM XEN R ECHE ACOR	RAOT R SCSM ACOR S GAOT ECHE OI	TBRF TURF DCA GONIA R TRBR S SPEN	
S-G 9	TURF DCA SCSM SPEN BAOT POC ASOL APAL	TURF DCA POR POC SPEN BAOT RDC TWOR	ANL TURF ACOR BAOT SPEN DCA POC CAL	ACOR BAOT SPEN GAOT AABR TWOR CAL DCA	BAOT TURF APAL XEN TWOR SCSM RAOT SARG	BAOT TWOR RAOT CAL SPEN SARG SCSM S	TBRF BAOT DCA TURF GONIA ACOR SPEN CAL	BAOT ACOR R TWOR CAL ECHE SARG BARN

7.4.1.1 Hard coral cover

Mean hard coral cover ranged between 0% at two SWR sites and 52.3 ± 5.2% (mean ± SE) at one of the LHI lagoon site (Fig. 7.3). Coral cover was consistently high at the SIMP midshelf island reefs (NWSI, SWSI & SSI), and ranged between 33% and 52% within the LHI lagoon sites (Fig. 7.3). Less than 20% cover was noted at: the two Cook Island sites; both sites adjacent to North Solitary Island; the exposed sites at LHI; and all the SWR sites except Black Rock. At the latter site, corals, particularly dendrophyllids (*Turbinaria* spp.), dominated the benthos (Fig.7.3 & 7.4).

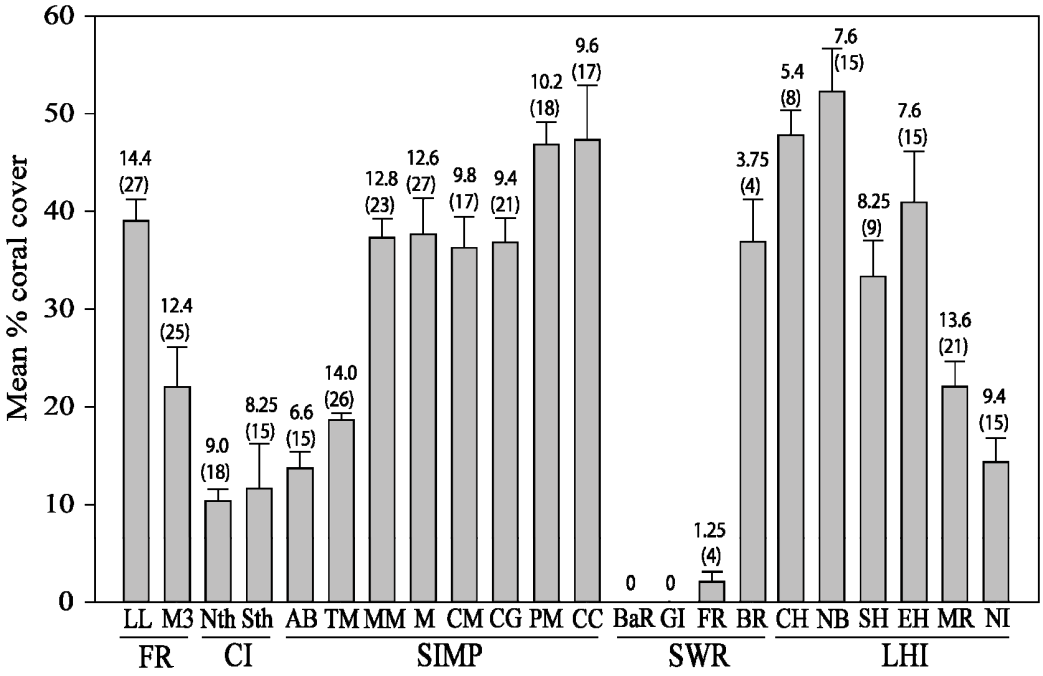

Figure 7.3: Mean percent hard coral cover (± SE) recorded at five subtropical eastern Australian locations: FR-Flinders Reef; CI-Cook Island; SIMP-Solitary Islands Marine Park; LHI-Lord Howe Island; and SWR-South West Rocks. Site acronyms are described in Figure 7.2. Mean coral species richness for each site is shown above the bars, with total richness at each site shown in parentheses.

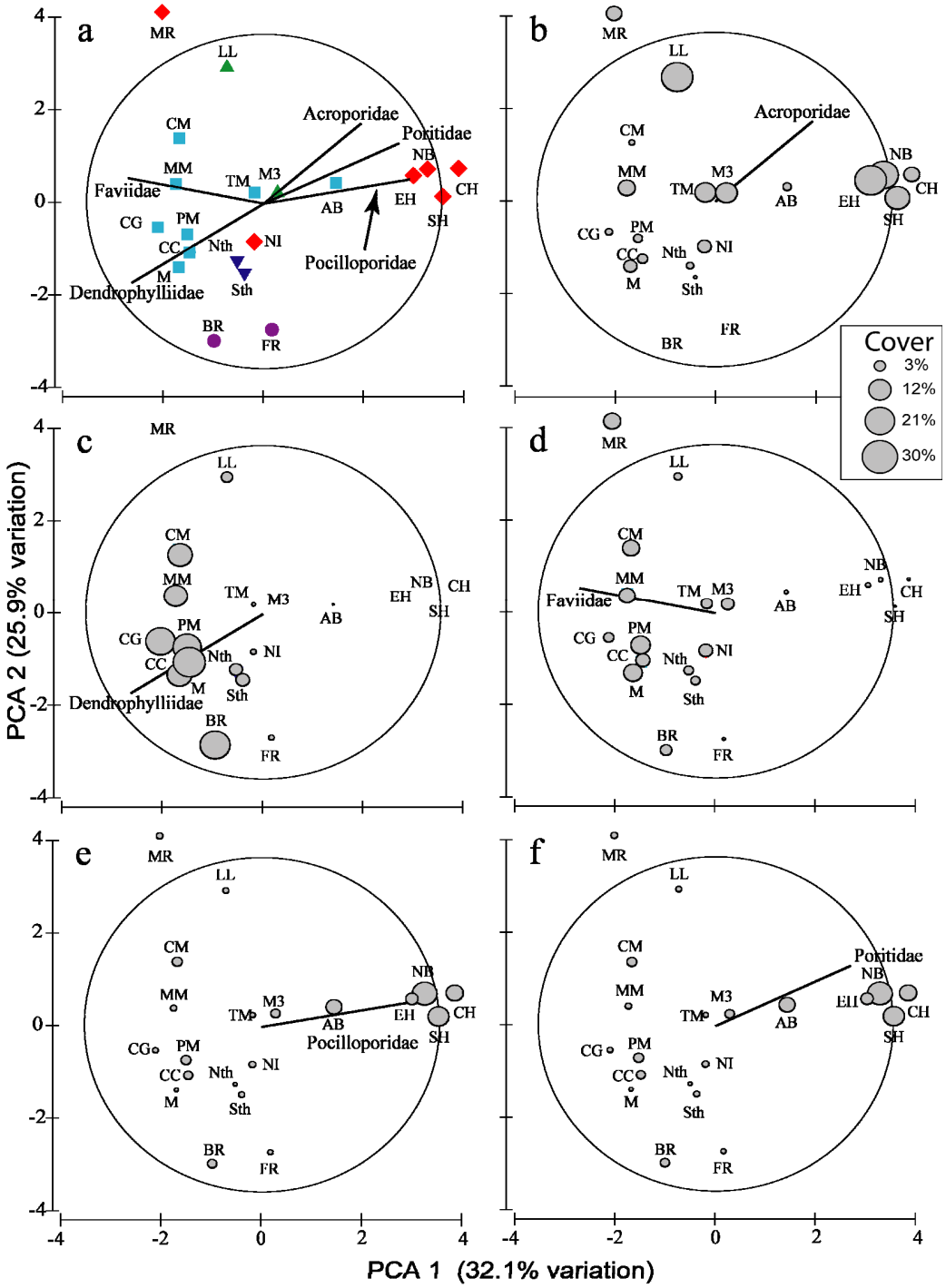

Figure 7.4: a) Principal component analysis (PCA) biplots of hard coral family assemblage data from subtropical sites: Flinders Reef - green triangles; Cook Island - blue triangles; SIMP - blue squares; SWR - purple circles; and LHI - red diamonds. Site acronym descriptions are given in Figure 7.2. Percent cover of each coral family represented by the overlayed bubble graph: b) Acroporidae; c) Dendrophylliidae; d) Faviidae; e) Pocilloporidae; and f) Poritidae.

All LHI lagoon sites orientated towards the right of the PCA biplot, with the midshelf island sites in the SIMP distributed to the left of the plot (Fig. 7.4a). Lord Howe Island lagoon sites were dominated by Acroporidae (Fig. 7.4b), Pocilloporidae (Fig. 7.4e) and Poritidae (Fig. 7.4f). In contrast, sites adjacent to SIMP midshelf islands were dominated by dendrophyllids with lower cover of Faviids (Fig. 7.5c, d).

The coral community at Anemone Bay was characterised by low cover (< 12%) of acroporids, pocilloporids and poritids. Trail Mooring, which is approximately 600 m away from Anemone Bay, orientated closer to Mooring No 3 (Flinders Reef) which lies 330 km away. Both of these sites had high acroporid cover, with a limited cover of pocilloporids and poritids (Fig. 7.4b, f). The orientation of Malabar Reef (LHI) within Figure 7.4 indicates no clear dominance by any coral family and its separation from the other sites is due to the presence of Agaricids, Pectinids and Merulinids, which were not observed at any other site. Reefs of SWR separated from all other locations and orientated toward the lower middle of the biplot (Fig. 7.4a). The coral community at Black Rock was dominated by dendrophyllids (Fig. 7.4c).

Results from the two-factor PERMANOVA indicated that, overall, there was a significant location effect for hard coral cover ($F_{4, 103} = 3.136$, $P = 0.039$), but small scale patterns (sites within location), displayed much stronger differences ($F_{17, 103} = 17.463$, $P = 0.001$). Pairwise contrasts indicated that only Flinders Reef and SWR were significantly different at the location level (Table 7.5a). However, at the site within location level, site differences were found within Flinders Reefs, SWR, between the lagoon and the exposed sites at LHI, and between NSI sites and all other sites investigated within the SIMP (Table 7.5b).

Table 7.5: Results from the pairwise comparisons for coral cover (CC) and coral richness (S) between a) location and b) sites within location. Significant values adjusted using Bonferroni corrections and shown in parentheses and are considered significant at the $p = 0.05$ level. Monte Carlo significance values are reported when insufficient unique permutations occurred and show by *. NT = no test. Significant values shown in bold.

a) Location (0.0125)	**CC**		**S**	
	t	***P***	***t***	***P****
FR, CI	2.174	0.150	5.848	0.020
FR, SIMP	0.395	0.704	0.718	0.486
FR, LHI	0.394	0.698	1.615	0.159
FR, SWR	1.451	0.224	4.031	**0.002**
CI, SIMP	2.555	0.035	1.085	0.322
CI, LHI	2.142	0.066	0.279	0.789
CI, SWR	0.092	0.941	3.180	0.032
SIMP, LHI	0.117	0.922	1.774	0.096
SIMP, SWR	2.883	**0.012**	7.226	**0.004**
LHI, SWR	2.466	0.031	4.831	**0.003**

b) Sites (Loc)		**CC**		**S**			**CC**		**S**	
Loc	**Sites**	**t**	***P***	**t**	***P****	**Loc**	**Sites**	**t**	***P***	**t**	***P****
FR (0.05)						**SIMP (0.007)**					
	LL, M3	3.635	**0.007**	0.358	0.754		AB, TM	2.623	0.034	4.994	**0.001**
CI (0.05)							AB, MM	9.040	**0.001**	4.616	**0.003**
	Nth, Sth	0.261	0.806	0.551	0.589		AB, M	5.833	**0.001**	5.695	**0.002**
							AB, CM	6.183	**0.001**	4.344	**0.001**
SWR (0.016)							AB, CG	7.638	**0.001**	2.577	0.026
	BaR, GI	NT	NT	NT	NT		AB, PM	11.46	**0.001**	4.542	**0.004**
	BaR, FR	1.852	0.097	2.623	0.037		AB, CC	5.715	**0.002**	2.354	0.054
	BaR, BR	8.383	**0.002**	28.86	**0.001**		TM, MM	8.947	**0.001**	0.593	0.568
	GI, BR	8.383	**0.001**	28.86	**0.001**		TM, M	5.011	**0.002**	0.755	0.484
	GI, FR	1.852	0.118	2.623	0.042		TM, CM	5.351	**0.002**	2.822	0.021
	BR, FR	7.699	**0.001**	2.763	0.034		TM, CG	7.026	**0.001**	2.659	0.032
							TM, PM	11.62	**0.001**	2.467	0.037
LHI (0.008)							TM, CC	5.059	**0.002**	2.350	0.040
	CH, NB	0.767	0.491	4.684	**0.005**		MM, M	0.079	0.932	0.083	0.939
	CH, SH	3.211	0.01	0.000	1.000		MM, CM	0.274	0.798	2.244	0.063
	CH, EH	1.181	0.282	3.534	**0.008**		MM, CG	0.148	0.894	2.143	0.068
	CH, MR	7.092	**0.001**	8.114	**0.001**		MM, PM	3.149	**0.007**	1.868	0.086
	CH, NI	9.417	**0.001**	5.645	**0.001**		MM, CC	1.681	0.127	1.853	0.089
	NB, SH	2.942	0.024	4.684	**0.003**		M, CM	0.277	0.785	2.945	0.024
	NB, EH	1.529	0.158	0.033	0.971		M, CG	0.148	0.894	2.481	0.026
	NB, MR	5.158	**0.001**	5.250	**0.002**		M, PM	2.100	0.081	2.376	0.042
	NB, NI	6.560	**0.001**	2.151	0.059		M, CC	1.435	0.203	2.063	0.085
	SH, EH	1.183	0.269	3.534	**0.006**		CM, CG	0.139	0.885	0.475	0.653
	SH, MR	2.481	0.048	8.114	**0.001**		CM, PM	2.668	0.034	0.645	0.517
	SH, NI	3.229	**0.003**	5.645	**0.001**		CM, CC	1.704	0.116	0.268	0.811
	EH, MR	3.229	0.014	4.819	**0.005**		CG, PM	2.946	0.015	0.824	0.428
	EH, NI	4.589	**0.002**	1.910	0.084		CG, CC	1.704	0.127	0.104	0.913
	NI, MR	2.148	0.069	3.115	0.014		PM, CC	0.078	0.951	0.569	0.602

7.4.1.2 Hard coral species richness

Hard coral species richness was highest at the exposed Flinders Reef site (Laurieland) and at Trail Mooring, which is adjacent to North Solitary Island (Fig. 7.3). Total richness (numbers in parentheses in Fig. 7.3) declined between Flinders Reef and Cook Island and then increased within the SIMP. Total species richness was generally higher at northern SIMP reefs (NSI and NWSI) compared to the more southerly sites (SWSI and SSI). There was an abrupt decline in total species richness between the SIMP and SWR, before rising at LHI. Results from univariate PERMANOVA analysis indicated there was a significant difference in mean species richness between location ($F_{4,103}$ = 16.448, $P < 0.001$) and between sites within location ($F_{17, 103}$ = 12.114, $P < 0.001$). Pairwise contrast showed that the difference between locations was driven by low numbers of corals species at SWR compared to all other locations (Table 7.5a). Within location contrasts showed that coral species richness at Flinders Reef and Cook Island was consistent over small spatial scales.

In contrast, the lack of coral presence at two of the SWR sites was the main driver of statistical differences at this location (Fig.7.3, Table 7.5b). At LHI, Malabar Reef species richness was significantly higher than all other sites, with difference also apparent between two lagoon sites, Comet's Hole and Stephen's Hole and most of the other sites (Table 7.5b). Anemone Bay recorded the lowest number of coral categories from all sites within the SIMP. Coral species richness on this reef was significantly lower than all sites except for Coral Gardens, which is located at SWSI and Coral Corner, which lies adjacent to SSI (Table 7.5b).

7.4.2 Temporal changes in benthic community composition in the SIMP

The orientation of the benthic assemblage centroids from eight sites investigated within the SIMP during 2004 and 2006 are shown in Figure 7.5a. Benthic communities associated with the reef adjacent to NWSI, SWSI and SSI (midshelf islands) orientated to the left of the ordination. Cluster analysis indicated that the benthic assemblages at these sites were more than 70% similar (Fig. 7.5a). In contrast, centroids for Anemone Bay and Trail Mooring (located at NSI) aligned to the top and bottom of the ordination, respectively. The ordination indicates that there was a distinct difference between years for most sites. For example, most centroids for the sites of NWSI, SWSI and SSI tended

Table 7.6: Results from multivariate three-factor PERMANOVA tests, which compared benthic community and coral community composition from eight sites located at four SIMP islands. Data were square-root transformed prior to analysis. Significant values shown in bold.

		Benthic community			Coral community		
Source	**df**	**MS**	**Pseudo-F**	***P*(PERM)**	**MS**	**Pseudo-F**	***P*(PERM)**
Year	1	2594.6	5.463	**0.018**	1849.8	2.633	0.088
Island	3	9876.9	2.917	**0.021**	15078	2.465	**0.048**
Site (Is)	4	2667.7	5.618	**0.001**	5642.2	8.032	**0.002**
Ye x Is	3	880.95	1.855	0.054	758.67	1.080	0.431
Ye x Site (Is)	4	474.87	1.366	0.022	702.46	1.272	0.144
Residuals	64	347.63			552.19		

Table 7.7: Results from pairwise PERMANOVA tests, which tested for differences in benthic community composition within sites between years (2004 vs 2006) at eight sites located at four islands within the SIMP using Type III sums of squares based on 999 permutations of residuals under a reduced model. Significant values shown in bold.

Islands	**Sites**	**T**	***P* (MC)**
North Solitary Island	Anemone Bay	2.054	**0.005**
	Trail Mooring	1.426	0.071
North West Solitary Island	Manta Mooring	1.657	**0.022**
	Midway Mooring	1.872	**0.009**
South West Solitary Island	Crazy Maze	1.863	**0.011**
	Coral Garden	1.713	**0.028**
Split Solitary Island	Pomfrey Point	1.430	0.058
	Coral Corner	0.932	0.520

to move towards the bottom of the nMDS in 2006, relative to their position in 2004. In contrast, at Anemone Bay and Trail Mooring, there was a shift to the right between subsequent survey dates, suggesting different types of changes in community composition between midshelf sites and those further offshore. Multivariate, three-factor PERMANOVA tests, using all replicate data, support these descriptions and showed a significant difference in benthic community composition between years, locations and sites within locations (Table 7.6). Furthermore, there was a significant year x site (island) effect. Pairwise comparisons which tested for differences within sites between years indicated that benthic community composition changed significantly at five of the eight sites investigated between 2004 and 2006 (Table 7.7).

Overall, a suite of benthic categories contributed to the significant difference in benthic community composition within sites between years. For example, 20 categories explained 50% of dissimilarity between years at Trail Mooring. Eight benthic categories that contributed the highest percentage of dissimilarity within each site between years are presented in Table 7.8. The significant assemblage shift at Anemone Bay was associated with at 100% increase in large anemones (*Entacmaea quadricolor*) and a consequent decline in sand, bare rock and rubble cover (Table 7.8). Additionally, an increase in dead coral with algae was noted, which may account for the decline in *Pocillopora damicornis* cover between years. A high proportion of change in benthic composition at Trial Mooring was driven by an increase in turfing algae and a decline in

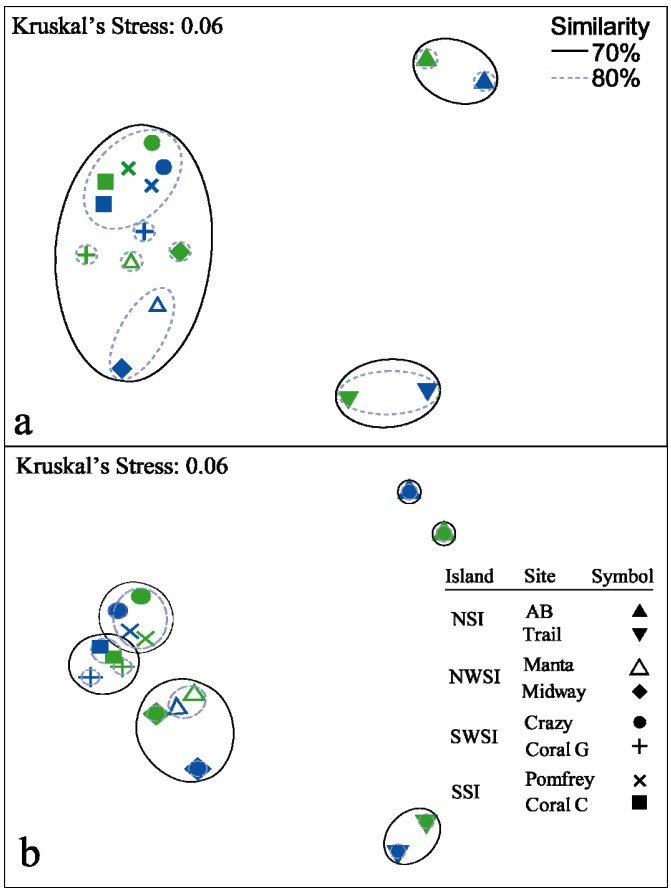

Figure 7.5: Non-parametric multidimensional ordination (nMDS) showing centroids for a) benthic community composition (n = 5 per site) and b) hard coral assemblages. Solid black and dashed grey contours encapsulate centroids that are at least 70 and 80% similar, respectively. Green and blue symbols represent 2004 and 2006 site centroids, respectively

Amphiroa anceps, *Corallina berteri* and coral taxa (Table 7.8). No clear pattern of change appears to be present when comparing the shift in benthic categories cover at the midshelf island sites (NWSI, SWSI and SSI). However, the cover of *Turbinaria* spp. tended to increase between 2004 and 2006, which accounted for approximately 3-5% dissimilarity at most midshelf island sites. Changes in the cover of sponge, soft coral, dead coral with algae and abiotic categories were also responsible for differences between years at these sites (Table 7.8).

7.4.2.1 Coral assemblage composition

The orientation of the coral assemblage centroids at each site within the SIMP was similar to the respective benthic composition centroids (Fig. 7.5b). The coral assemblage at each site grouped at the 70% level within each island location except for the sites at NSI. Coral assemblage composition showed significant small-scale differences (sites nested within location) and, as indicated by the non-significant interaction tests, this pattern of change was consistent throughout the marine park (Table 7.6). Yearly differences in coral community composition were not significant, which indicates the stability of the coral assemblage at all sites through time (Table 7.6). Results from pairwise PERMANOVA tests, which examined differences in coral assemblages between islands, and sites within islands, indicated that the overall sites within location difference was due to the significant difference between Anemone Bay and Trail Mooring (T = 4.35, *P*(MC) = 0.004). All other pairwise comparisons (locations and sites within locations) were not significantly different, indicating that the coral composition was similar at sites within islands except at NSI.

7.4.3 Decadal change in subtropical benthic community composition

Overall, hard coral cover on east Australian subtropical reefs was similar in 2005-2006 as was observed in the 1990s. During the present study, mean hard coral cover ranged between 10.96% (Cook Island) and 52.27% (NBW, LHI) averaging 32.85% ± 3.86 (± SE). Similarly, hard coral cover at these sites during the 1990s averaged 33.57% ± 3.65 and ranged between 7.65% (Cook Island) and 50.60% (EH, LHI). However, there was a notable temporal differences in the cover of some categories, including an overall increase in algal cover (23.58% ± 5.91 to 31.65% ± 5.32) and a decline in substratum cover (26.23% ± 3.01 to 19.11% ± 5.20) between subsequent decades (Table 7.9).

Table 7.8: Results of SIMPER analysis indicating the eight benthic categories that contributed the highest proportion of dissimilarity (% DIS) within sites between years. Values below years indicate mean percent cover for each category.

Sites		% Cover 2004	% Cover 2006	% DIS	Sites		% Cover 2004	% Cover 2006	% DIS
North Solitary Island									
Anemone Bay	Large anemone	14.06	28.30	6.73	**Trail Mooring**	*Amphiroa anceps*	1.51	1.17	3.52
	Sand	1.88	0.00	5.88		Turf algae	8.70	15.44	3.34
	Bare rock	3.72	0.85	5.35		*Corallina berteri*	2.34	1.04	3.25
	Rubble	7.40	2.34	5.14		*Favites abdita*	1.39	0.30	3.17
	Dead coral with algae	2.16	6.30	4.52		Sand	1.30	0.08	2.91
	Sponge encrusting	2.25	0.30	4.11		*A.* sol/glau/hyac	0.58	0.53	2.75
	P. damicornis	8.01	6.00	3.77		Recently dead coral	0.15	1.42	2.68
	Old dead coral	1.14	0.18	3.57		*Acropora* cor/cas	0.90	0.42	2.43
North West Solitary Island									
Manta Mooring	Zoanthid	0.90	2.22	4.86	**Midway Mooring**	Rubble	3.61	0.14	4.93
	Recently dead coral	0.01	2.19	4.51		Soft coral massive	0.35	3.57	4.23
	A. sol/glau/hyac	1.99	6.05	4.08		Sand	5.11	9.67	4.2
	Soft coral massive	0.98	4.45	3.81		Dead coral algae	2.02	6.76	3.81
	M. magnistellata	1.54	0.59	3.45		Sponge submassive	3.20	0.71	3.44
	Sediment	3.50	0.94	3.23		Sponge encrusting	2.40	0.29	3.31
	Bare rock	0.29	1.82	2.90		*M. magnistellata*	0.62	2.53	3.23
	Sand	3.06	4.80	2.72		Soft coral encrusting	1.17	0.04	2.88
South West Solitary Island									
Crazy Maze	Rubble	5.57	1.46	5.27	**Coral Garden**	Dead coral algae	2.25	8.88	5.44
	Sponge encrusting	6.76	2.56	5.10		Sediment	3.65	0.66	4.4
	Turbinaria fron/men	16.40	16.89	4.47		Turf algae	23.14	14.82	3.93
	Coralline algae	10.24	16.97	4.16		*Turbinaria* fron/men	14.14	23.33	3.84
	P. superficialis	0.61	0.00	3.47		Sand	9.49	8.58	3.22
	Green algae other	1.35	0.18	3.40		Bare rock	1.85	4.84	3.13
	Recently dead coral	0.01	0.64	3.31		Brown algae other	0.81	0.03	3.04
	Old dead coral	0.52	0.00	3.23		Sponge submassive	1.54	0.19	3.04
Split Solitary Island									
Pomfrey Point	*A.* sol/glau/hyac	2.28	0.66	4.98	**Coral Corner**	*Turbinaria* fron/men	30.03	29.05	6.04
	Dead coral algae	3.06	7.56	4.27		Ascidian solitary	6.30	5.95	4.50
	Rubble	2.13	0.23	4.24		Sand	4.00	1.61	4.43
	Barnacle	0.10	0.85	3.22		Dead coral algae	3.13	6.71	3.66
	Green algae other	1.88	0.40	3.13		Sponge encrusting	1.96	3.92	3.42
	Turbinaria fron/men	20.43	22.28	2.97		Rubble	1.21	0.52	3.18
	Soft coral encrusting	0.26	1.06	2.87		Soft coral encrusting	0.90	1.23	3.12
	Acan. lordhowensis	0.64	0.08	2.79		Turf algae	11.22	9.24	3.03

Table 7.9: Summary of decadal comparisons in mean cover of benthic categories associated with subtropical island reefs extending along the east coast of Australia.

Benthic categories	Flinders Reef		Cook Island		Solitary Islands Marine Park							
					NSI		NWSI		SWSI		SSI	
	1994[a]	2005[f]	1997[b]	2006[f]	1992[c,d]	2006[f]	1992[c,d]	2006[f]	1992[c,d]	2006[f]	1992[c,d]	2006[f]
Acroporidae	21.50	20.53	2.70	0.79	16.51	7.10	4.5	6.30	9.60	1.10	6.63	2.40
Agariciidae	0.20	0.03	0.00	0.00	0.00	0.00	0.00	0.00	0.00	0.03	0.00	0.00
Dendrophylliidae	1.40	1.97	0.20	5.54	0.00	0.23	8.12	18.70	15.88	24.12	17.28	30.23
Faviidae	1.80	3.47	1.85	2.71	0.65	2.20	6.30	9.83	11.20	6.40	6.15	9.33
Merulinidae	0.05	0.63	0.00	0.00	0.00	0.10	0.00	0.13	0.00	0.03	0.00	0.00
Mussidae	0.40	0.10	0.70	0.17	0.40	0.10	0.00	0.60	0.00	0.83	1.275	0.47
Pectinidae	0.00	0.00	0.00	0.00	0.00	0.00	0.00	0.00	0.00	0.03	0.00	0.00
Pocilloporidae	2.55	1.90	1.05	0.79	9.75	4.53	4.09	0.83	5.33	2.03	2.93	2.80
Poritidae	0.30	1.27	0.00	0.92	1.03	1.80	1.96	0.93	5.75	1.60	0.04	1.37
Siderastreidae	0.00	0.57	1.15	0.04	0.00	0.03	0.0	0.10	0.00	0.27	0.00	0.40
Hard corals other	3.90	0.00	0.00	0.00	0.00	0.00	0.00	0.00	0.00	0.00	0.00	0.00
Hard coral total	**32.30**	**30.47**	**7.65**	**10.96**	**32.40**	**16.10**	**24.96**	**37.43**	**47.75**	**36.45**	**34.65**	**47.03**
Soft coral	**14.60**	**19.07**	**3.75**	**8.58**	**0.90**	**0.73**	**7.20**	**5.30**	**1.60**	**0.37**	**7.10**	**2.53**
Algae total	**31.45**	**32.37**	**67.00**	**57.46**	**5.20**	**49.77**	**28.00**	**29.97**	**4.10**	**29.36**	**44.00**	**22.73**
Seagrass	**0.00**	**0.00**	**0.00**	**0.00**	**0.00**	**0.00**	**0.00**	**0.00**	**0.00**	**0.00**	**0.00**	**0.00**
Invertebrates	**15.30**	**10.63**	**15.60**	**9.59**	**2.50**	**19.73**	**9.30**	**5.40**	**5.60**	**9.60**	**5.20**	**14.90**
Substratum	**6.30**	**7.44**	**4.55**	**13.42**	**59.40**	**13.63**	**25.10**	**21.87**	**36.00**	**24.16**	**9.40**	**12.73**

Benthic categories	Lord Howe Island										South West Rocks	
	CH		NBW		SH		EH		MR			
	1993[e]	2005[f]	1993[e]	2005[f]	1993[e]	2005[f]	1993[e]	2005[f]	1993[e]	2005[f]	1997[b]	2006[f]
Acroporidae	0.00	6.73	5.50	24.80	21.50	17.20	33.70	28.67	7.00	6.53	0.00	0.00
Agariciidae	0.00	0.00	0.00	0.00	0.00	0.00	0.00	0.00	0.00	0.53	0.00	0.00
Dendrophylliidae	0.00	0.00	0.00	0.00	0.00	0.00	0.00	0.00	1.30	0.00	18.35	15.42
Faviidae	0.00	0.20	0.80	0.60	0.80	0.13	0.40	0.73	8.00	9.67	1.95	2.25
Merulinidae	0.00	0.00	0.00	0.00	0.00	0.00	0.00	0.00	0.50	1.87	0.00	0.00
Mussidae	0.00	0.00	0.00	0.20	0.00	0.00	0.20	0.00	3.50	0.07	0.00	0.00
Pectinidae	0.00	0.00	0.00	0.00	0.00	0.00	0.20	0.00	0.60	0.33	0.00	0.00
Pocilloporidae	16.40	9.60	16.00	20.20	6.40	14.40	6.40	5.07	1.60	1.40	3.75	1.75
Poritidae	27.90	31.27	2.40	6.47	16.70	1.60	9.40	6.47	6.50	1.60	0.00	0.00
Siderastreidae	0.00	0.00	0.00	0.00	0.00	0.00	0.00	0.00	0.00	0.07	0.00	0.00
Hard corals other	0.00	0.00	0.50	0.00	0.20	0.00	0.30	0.00	0.10	0.00	0.00	0.00
Hard coral total	**44.30**	**47.80**	**25.20**	**52.27**	**45.60**	**33.33**	**50.60**	**40.93**	**29.10**	**22.07**	**24.05**	**19.42**
Soft coral	**0.00**	**2.07**	**2.40**	**3.73**	**24.00**	**21.13**	**20.20**	**27.53**	**12.40**	**3.00**	**3.65**	**0.25**
Algae total	**19.70**	**13.40**	**11.70**	**3.20**	**10.80**	**10.00**	**8.60**	**14.33**	**33.20**	**67.60**	**22.45**	**49.67**
Seagrass	**0.00**	**0.00**	**1.10**	**1.00**	**0.00**	**2.27**	**0.20**	**0.00**	**0.00**	**0.00**	**0.00**	**0.00**
Invertebrates	**4.60**	**7.93**	**1.40**	**0.53**	**0.90**	**1.20**	**1.60**	**1.13**	**0.00**	**3.73**	**26.20**	**14.33**
Substratum	**31.20**	**28.80**	**58.80**	**39.27**	**18.70**	**32.07**	**18.70**	**16.07**	**25.30**	**3.60**	**21.30**	**16.33**

[a] Harrison *et al.* (1998) Data pooled from two sites, mean cover determined from eleven 30 m transects located between 5-10 m depth.
[b] Harriott *et al.* (1999) Data pooled from two sites, mean cover determined from ten 20 m transect located between 5-8 m depth.
[c] Harriott *et al.* (1994) Mean percent cover determined from four 20 m transect located between 5-9 m depth at each island site.
[d] Harriott *et al*. unpublished data
[e] Harriott *et al.* (1995) Mean cover determined at each site from four 50 m or 30 m transects.
[f] Present study: Flinders Reef, Cook Island, SIMP, SWR - data pooled within locations from two sites containing five 30 m transects

At the site level, some changes in benthic composition are apparent. For example, hard coral cover declined at two SIMP locations, NSI and SWSI and at Erscott's Hole (LHI). There was also an increase in invertebrate and substratum cover at NSI and an increase in algal cover at both SWSI and Erscott's Hole (Table 7.9). The cover of acroporids and pocilloporids declined by over 50% at NSI, with an increase in the cover of Faviids noted (Table 7.9). A decline in acroporid and faviid cover was noted at SWSI but, at this island, corals from the family Dendrophylliidae increased through time. At Erscott's Hole, the shift in coral community composition paralleled that at NSI. In

contrast, coral cover increased at NWSI and SSI within the SIMP, and NBW a LHI lagoon site (Table 7.9). This increase in coral cover was attributed to the doubling of dendrophyllids at the SIMP midshelf island reefs and an increase in the cover of acroporids, pocilloporids and poritids at NBW (Table 7.9). At Malabar Reef (exposed LHI site), a 100% increase in algal cover contributed to the decline in hard coral, soft coral and substratum categories.

7.5 Discussion

Subtropical island-associated reefs, located south of the GBR in eastern Australia are dominated by scleractinian corals. This study revealed strong latitudinal differences in benthic and coral assemblages, and interestingly, community composition at some sites was more similar to those hundreds of kilometres away than to that of neighbouring reefs. Within the SIMP, a significant shift in benthic composition was shown at some sites through time; however, the coral community remained consistent over a 3 year period. Decadal comparisons showed that hard coral cover was generally stable at a regional scale, but small-scale differences within sites were apparent.

7.5.1 Latitudinal variation in benthic community composition

This study showed a significant regional difference in benthic community composition with some interesting similarities evident between locations that were separated by hundreds of kilometres, as well as a significant difference in assemblage composition over small spatial scale (< 1 km). For example, the benthic community at Flinders Reef was more similar to that at the reef crest sites at LHI (Erscott's Hole and Stephen's Hole) than the geographically closer Cook Island assemblages. At Flinders Reef, and along the LHI reef crest, a high cover of *Acropora* spp. was recorded. In contrast, the benthic assemblage at Cook Island was dominated by marine algae, and shared 65% similarity to the exposed LHI sites (Fig. 7.2). This resemblance may be due to a number of physical factors including wave exposure and nutrient availability at these locations. Benthic communities at Cook Island, which is located approximately 4 km south east of the Tweed River, are regularly exposed to terrigenous discharge following storm events. The direction of the freshwater plume into the marine environment is determined by the strength of local wind and wave action and current direction, particularly the East

Australian Current (EAC), which generally deflects riverine waters from the Tweed River to the south (Davies 2005; Rule *et al.* 2007). Additionally, the combination of the southward flowing EAC current and the narrowing of the NSW continental shelf results in the formation of a thermal fronts along the nearshore zone adjacent to Tweed Heads, Cape Byron and South West Rocks (Oke and Middleton 2000; Roughan *et al.* 2003; Roughan and Middleton 2004). These fronts regularly transport cool upwelled, nutrient-rich waters in a northward direction, resulting in highly productive regions, which facilitate phytoplankton and macroalgal growth. Similarly, exposed reefs communities at LHI are regularly subjected to dominant south to south-easterly sea conditions; this generates a dynamic environment with a constant supply of nutrients from northward flowing waters and upwellings associated with the Lord Howe Seamount (Environment Australia 2002). Harriott and Banks (2002), suggested that increased nutrients, from periodic pulses of terrigenous discharge and upwelling events, stimulate algal growth along the NSW coast. This limits coral settlement and enhances the growth of macroalgae and other competing sessile invertebrates. These competing organisms potentially affect coral calcification and growth (through bioerosion), limit coral recruitment (limit suitable substratum) and reduce the survival of new coral recruits.

Wave energy is another important physical factor controlling sublitoral marine communities (Dollar 1982; Jokiel *et al.* 2004). Studies have demonstrated a strong correlation between wave energy and coral distribution (Dollar and Grigg 2004; Storlazzi *et al.* 2005). Jokiel *et al.* (2004) demonstrated that coral cover, diversity and species richness in Hawaii (a subtropical location), were all negatively correlated with maximum wave height and wave direction. Benthic communities differ according to pattern of wave exposure, and wave energy is a dominant influence in cross-shelf benthic patterns along the east coast of Australia. Along the northern NSW coast, wave heights of the dominant south easterly seas can exceed 6 m during unstable climatic conditions, with a maximum height of > 13 m being recorded in the past 10 years (Manly Hydraulics Laboratory 2007).

Wave energy may have various impacts on benthic communities depending on the depth of the reef and its topography. Shallow habitats are susceptible to heavy wave action but this influence can be modified by reef topography, geometry and aspect (Jokiel *et al.* 2004; Storlazzi *et al.* 2005). The structural complexity of reefs can provide small-scale

niches for fragile organisms, such as hard corals. For example, the LHI lagoon affords protection from wave disturbance, and supports a high cover of hard corals compared to the exposed sites on the north and eastern side of the island. However, coral species richness was highest at the LHI exposed sites, which suggest that diversity may be highest at locations that are exposed to periodic disturbances (i.e. intermediate disturbance hypothesis; Connell 1978). The acquisition of small-scale physico-chemical data to complement existing biological data would enable a clearer understanding of the relationship between bottom-up and top-down controlling mechanisms and patterns in benthic community composition associated with eastern Australia subtropical reefs.

7.5.1.1 Coral community composition

Intra-location variation in coral community composition was found to be greater than variation between localities. Coral cover varied significantly between sites within Flinders Reef, between lagoon reefs and the exposed sites at LHI, between midshelf islands and the offshore island within the SIMP, and between sites at SWR. This pattern of spatial variance agrees with previous studies which found that coral cover varies significantly over similar spatial scales. For example, in a hierarchical study along the Florida Reef Tract Murdoch and Aronson (1999) demonstrated low variance among sites within reefs (< 2 km apart), much greater variance between reefs that were 10-20 km apart, and only marginal differences between sectors up to 100 km apart. North Solitary Island lies between 15-40 km north-northeast of the other SIMP islands and coral cover and composition (pocilloporid and acroporid dominated) at this location was significantly different to that found at the midshelf islands (dendrophyllid and faviid dominated; Fig. 7.4). Conversely, coral cover and species composition at Mooring No 3 (Flinders Reef) was more similar to Trail Mooring (NSI) than Laurieland which is on the opposite side of Flinders Reef (Fig. 7.3 and 7.4). At SWR, coral cover was significantly higher at Black Rock compared to all other SWR sites, yet the sites are less than 2 km from each other. The benthic community at Black Rock appears unique at this location due to the relatively high coral cover compared to all other sites, and was more similar to the SIMP midshelf island sites (Fig. 7.4). Interestingly, coral species richness at SWR was significantly lower than at all other locations. This abrupt decline in coral cover in combination with a significant reduction in species richness south of the SIMP may indicate the limited or sporadic connection between SWR and northern

locations or the biogeographical limits of many subtropical and tropical species (Harriott and Banks 2002).

Pattern of coral cover and differences in species richness found during this study may be a result of the difference in magnitude of both environmental and biological factors acting in isolation or in synergy at different spatial scales. Small-scale spatial variability in coral assemblages may be attributed to the biological variability within the coral species present at different location. Previous research at Australian subtropical locations has shown that corals exhibit interspecific differences in morphology, fragmentation rates, dispersal patterns, reproductive mode, recruitment rate and survivorship relative to different levels of exposure and other disturbances (Harriott 1992; Harriott and Banks 1995; Wilson 1998; Wilson and Harrison 1998; Carroll 2001; Harriott and Banks 2002; Wilson and Harrison 2003; Wilson and Harrison 2005). For example, acroporids and pocilloporids dominate the coral community at NSI whereas dendrophyllids, which are generally associated with regions of high turbidity, dominate reefs closer to shore (Done 1982; Harriott *et al.* 1994). These differences may be attributed to the limited light regime at midshelf southern reefs relative to the northern offshore island reefs. Water clarity and light penetration tends to be higher further offshore due to the stronger influence of the EAC and distance from nearshore processes. The dominance of dendrophyllids, and colony morphology (i.e. horizontal growth forms) at SSI, SWSI and NWSI suggest that midshelf reefs are light limited. This may be due to increased suspended sediment and algal blooms caused by northern flowing nutrient rich waters mixing with warmer southward flowing currents and proximity to freshwater runoff from the adjacent coast. *Turbinaria mesenterina* and *T. frondens* occur in turbid locations over a wide geographical area (Veron 2000b) and are found on rocky substrata at subtropical and temperate latitudes on both the east and west coasts of Australia (Harriott *et al.* 1994; Veron 2000b). During manipulative experiments, Sofonia and Anthony (2008) demonstrated that *T. mesenterina* is well adapted to high sediment regimes, showing a high tolerance to sediment loads an order of magnitude greater than that found under the most severe natural conditions. They are therefore able to flourish in turbid/low light environments. This is consistent with the results of this study that found that *Turbinaria* species are associated with subtropical

benthic communities where light is a limiting factor due to the highly turbid waters found along the NSW coast (personal observations, Chapter 6).

The higher abundance of *Acropora* species at NSI compared to other reefs in the SIMP may be due to the increased influence of the southward flowing EAC, which has been hypothesised to provide a vehicle for recruitment of broadcast spawning *Acropora* coral species from northern reefs such as Flinders Reef (Wilson and Harrison 1998). Indeed, seawater temperature at this offshore island tends to be 1-2ºC above those recorded at the midshelf islands (Chapter 5), which suggests a greater EAC influence. Wilson and Harrison (2003) observed asynchronous spawning of 24 coral species at the northern islands in the SIMP and suggested the potential for successful recruitment of planulae larvae during favourable oceanic conditions. However, they indicated that recruitment at high latitude reefs is restricted by the limited release of gametes, reduced fertilisation rates, and the sporadic nature of the dominant currents, which may restrict settlement of NSI spawned corals further south. Additionally, Hughes *et al.* (2002) found a 20-fold decline in recruitment of broadcast spawning species with increasing latitude along eastern Australia. In contrast, brooding species, such as pocilloporids, had a higher potential for recruitment at high latitude reefs.

Of the sites investigated reef accretion only occurs at LHI, where a fringing reef has formed over a geological time scale on the western side of the island. In contrast, corals along the mainland of subtropical eastern Australia form a veneer over the rocky substratum, and true coral reefs have not formed (Veron 1993). Harriott and Banks (2002) proposed a qualitative model for the factors and processes that influence the southward attenuation of corals and coral reefs. Comparing the biological-physical conditions seen at LHI, where reef accretion has occurred, to those on reefs associated with mainland Australia, several processes and factors appear to facilitate reef accretion. Firstly, the coral assemblage within the lagoon is composed of relatively fast-growing staghorn acroporids and brooding pocilloporids. These acroporids, including *Acropora yongei* and *A. lovelli*, have over geological time, provided the framework for fringing reef development on the western side of the island. The geology of the island also provides protections from the dominant south-easterly sea conditions. Woodroffe *et al.* (2006) indicated that LHI is situated at the critical Darwin Point (a threshold of atoll

formation, [Grigg 1982]), where the island is undergoing a shift from truncation by wave action to accumulation of reef and associated carbonates. The shallow nature of the lagoon provides adequate insolation for photosynthesis by zooxanthellae. In contrast, subtropical reefs adjacent to mainland Australia are regularly exposed to large storm events which cause fragmentation of corals and increased erosion of coral skeleton. Additionally, due to limited aragonite deposition, many of the coral species present at these locations have reduced growth rates (Harriott 1999). Periodic exposure to large storm events results in fragmentation and coral loss on exposed reefs, as well as protracted periods of turbid water and low light intensity.

7.5.2 Temporal pattern in SIMP community composition

Monitoring benthic community composition over yearly temporal scales within the SIMP indicates that most of the within site variance was explained by benthic categories other than hard corals. Thus, while there was a significant temporal change in benthic community structure, this was mostly associated with taxa other than corals. For example, at Anemone Bay, a 100% increase in the cover of large sea anemone was observed (Table 7.8). *Entacmaea quadricolor* (bubble-tip anemone) dominates the small boulder field adjacent to the survey area, and this anemone field has substantially increased in size over the past 10 years. Scott *et al.* (In review) also noted an increase in anemone cover within the bay, from 10.7 to 58.9 % between 1994 and 2008. This increase in anemone cover may be attributed to the sexual and asexual strategies of this species and the favourable conditions found within the northward facing bay (Scott *et al.* in review and references therein). Further research is required to understand the flow-on effects associated with increased space pre-emption by this dominant benthic organism, as competition with other sessile species may lead to a further loss in hard coral cover through time.

This study was conducted during a period when seawater temperatures did not exceed predicted SIMP bleaching thresholds for more than one week and large storm events that result in coral damage did not occur (Manly Hydraulics Laboratory 2007). However, minor bleaching and mortality associated with Australian subtropical white syndrome was observed (see previous chapters). The scales of variation found within sites between monitoring periods may indicate the level of natural variability within the

community. Habitat heterogeneity is a characteristic of subtropical reefs along eastern Australia (Harriott *et al.* 1994); this manifests as small-scale differences in bottom topography that affect other physical parameters such as water movement and light intensity at small spatial scales (Murdock and Aronson 1999). However, the coral community composition remained relatively stable between 2004 and 2007 (Table 7.6). Small-scale, within habitat variation is an important and consistent component of the ecology of subtropical reefs. An understanding of levels of natural variation in assemblage dynamics, which were observed during this study, is required before studies can detect community shifts that have resulted from human-induced disturbances such as climate-change-related effects and disease outbreaks. This study provides information on the natural variation in benthic and coral community composition within the SIMP during periods of minimal external stressors and provides a baseline for future studies following periods of perturbation.

7.5.3 Decadal changes in community composition

Comparisons between this study and research completed during the early 1990s demonstrated a change in benthic community structure over the past 10 years. However, it is difficult to determine if the observed changes are due to: i) natural or anthropogenic influences; ii) community shifts due to small-scale variability within each site; or iii) due to natural successional changes (i.e. equilibrium theory). During the present study, high coral cover was the main criteria for site selection, and following rapid assessment dives, each site was positioned within 10-14 m depth, except for in the LHI lagoon. In contrast, during the 1990s surveys, sites were positioned in 5-10 m depth which, as indicated by Harriott *et al.* (1994), were areas of highest coral cover at that time. Therefore, it appears that there may have been a transition of coral dominance from shallower (< 10 m) to deeper depths at subtropical reefs along the east coast of Australia. This change in coral dominance to deeper water has possibly led to a shift in corals species composition with the current assemblages comprising of a suite of species that are more tolerant to lower light conditions. For example, at most site evaluated during the 1990 branching acroporids and pocilloporids contributed a high proportion coral cover; in contrast, a higher occurrence of dendrophyllids was recorded during this study.

A loss of hard coral cover at shallow sections of the reefs within the SIMP may be associated with large storm events which occurred prior to beginning of the present study. During a large storm event in 2003 many branching, plate and encrusting corals were removed from the substratum at shallow reefs throughout the SIMP, including areas previously studied by Harriott *et al.* (1994) (S. Smith personal communication). Large storm events are a regular event along the northern NSW coast leading to the loss of coral cover. Three major storm events occurred during autumn 2009 and resulted in the damage and loss corals at many reefs within the SIMP. It has been estimated that increased turbidity and wave exposure may have caused up to 20% coral loss at midshelf reefs within the SIMP (preliminary findings). Additional surveys are currently underway to determine the effect of these recent storm events over larger spatial scales along the NSW and southern Queensland coast.